The Journal of PHARMACOLOGY And Experimental Therapeutics

Fentanyl but not Morphine Interacts with Nonopioid Recombinant Human Neurotransmitter Receptors and Transporters

Randy Torralva, Amy J. Eshleman, Tracy L. Swanson, Jennifer L. Schmachtenberg, William E. Schutzer, Shelley H. Bloom, Katherine M. Wolfrum, John F. Reed, and Aaron Janowsky

Research Service, VA Portland Health Care System, Portland, Oregon (R.T., A.J.E., T.L.S., J.L.S., W.E.S., S.H.B., K.M.W., J.F.R., A.J.); Coda Research, Portland, Oregon (R.T.); Departments of Psychiatry (R.T., A.J.E., T.L.S., J.L.S., W.E.S., S.H.B., K.M.W., J.F.R., A.J.), Behavioral Neuroscience (A.J.E., A.J.), Oregon Health & Science University, Portland, Oregon; and The Methamphetamine Abuse Research Center, VA Portland Health Care System and Oregon Health & Science University, Portland, Oregon (W.E.S., A.J.)

ABSTRACT

Synthetic opioids, including fentanyl and its analogs, have therapeutic efficacy in analgesia and anesthesia. However, their illicit use in the United States has increased and contributed to the number one cause of death for adults 18–50 years old. Fentanyl and the heroin metabolite morphine induce respiratory depression that can be treated with the μ opioid receptor (MOR) antagonist naloxone. With higher or more rapid dosing, fentanyl, more than morphine, causes chest wall rigidity and can also induce rapid onset laryngospasm. Because non-MORs could mediate differing clinical manifestations, we examined the interactions of fentanyl and morphine at recombinant human neurotransmitter transporters, G protein–coupled receptors, and the N-methyl-D-aspartate glutamate receptor. Both drugs were agonists at MOR, κ, and δ opioid receptors. Morphine had little or no affinity at other human receptors and transporters (K_i or IC_{50} value >100 μM). However, fentanyl had K_i values of 1407 and 1100 nM at α_{1A} and α_{1B} adrenoceptor subtypes, respectively, and K_i values of 1049 and 1670 nM at dopamine D4.4 and D1 receptor subtypes, respectively; it also blocked [^{3}H]neurotransmitter uptake by the vesicular monoamine transporter 2 (IC_{50} = 911 nM). Pharmacokinetic models indicate that these Ki and IC_{50} values are pharmacologically relevant. Fentanyl had little affinity for other receptors or transporters. Thus, noradrenergic disposition at specific receptor subtypes in relevant organs may play a role in respiratory and cardiothoracic effects of fentanyl. Data suggest that less selective fentanyl receptor pharmacology could play a role in the different clinical effects of morphine compared with fentanyl, including fentanyl-induced deaths after illicit use.

SIGNIFICANCE STATEMENT

The synthetic opioid fentanyl induces different clinical effects, including rapid onset muscular rigidity, vocal cord closure, and rapid death, than the heroin metabolite morphine. Our data indicate for the first time that the two drugs have very different effects at recombinant human neurotransmitter receptors and transporters that might explain those clinical differences.

Introduction

Fentanyl (N-phenyl-N-[1-(2-phenylethyl)-4-piperidinyl] propanamide), a synthetic opioid, and its analogs (F/FAs) are involved in almost twice as many opioid-induced deaths as heroin (diacetyl morphine), the metabolic precursor of morphine ((Hedegaard et al., 2018); Jannetto et al., 2019). However, in hospitals, fentanyl use for analgesia and anesthesia is routine (Stanley, 2014). Side effects include respiratory depression that is treated with naloxone, a μ opioid receptor (MOR) antagonist. Additionally, fentanyl-induced severe skeletal muscle rigidity

(FIMR) of the chest wall and diaphragm and acute vocal cord closure (laryngospasm) require a muscle relaxant/paralytic and endotracheal intubation to restore adequate ventilation. These fentanyl-induced respiratory effects (FIRE) may play a role in rapid death associated with illicit fentanyl use.

Symptoms of overdose from illicit use of heroin similarly include naloxone-reversible respiratory depression. However, patients who overdose after illicit fentanyl exposure are far less likely to recover even after treatment with naloxone (Slavova et al., 2017), and higher doses of naloxone are generally required (Somerville et al., 2017). This reduced sensitivity to naloxone could be because of non–MOR-related effects of fentanyl and may explain why deaths from F/FAs continue to increase (Baumann et al., 2018). In fact, naloxone in higher doses causes noncardiogenic pulmonary edema (Jiwa et al., 2018), exacerbating respiratory failure and non–MOR-mediated symptoms of opioid overdose. Rapidity of injection and dose of fentanyl are the key determinants of the incidence, severity, and duration of FIRE (Grell et al., 1970). Symptoms occur within 2 minutes of drug injection and
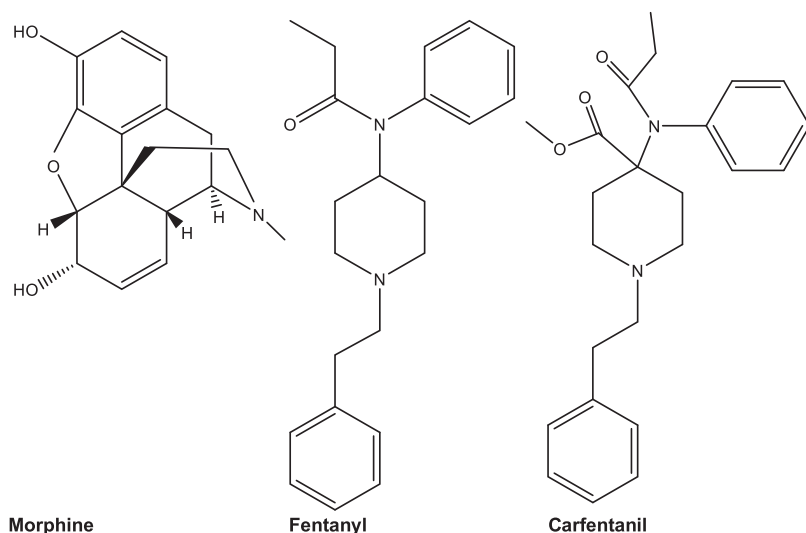
Fig. 1. Structures of morphine, fentanyl, and carfentanil.

can last up to 15 minutes (Scamman, 1983; Streisand et al., 1993). Fentanyl's inactive metabolite, norfentanyl, appears in plasma within 90 seconds of a bolus intravenous injection (McClain and Hug, 1980), but little norfentanyl is found in autopsy tissue from overdose deaths because of fentanyl (Burns et al., 2016). The absence of metabolite suggests that death from a bolus injection of fentanyl is rapid, distinguishing it from respiratory depression after heroin overdose.

Complex fentanyl pharmacokinetics vary across compartments (plasma, cerebrospinal fluid, brain lipid) (Peng and Sandler, 1999). Although fentanyl plasma concentrations are much lower than brain lipid concentrations (Chesser et al., 2019), the high lipid solubility and rapidity of exposure to the CNS after high-dose fentanyl suggests that micromolar K_i values for fentanyl binding to non-MORs could be relevant under toxic conditions (Stone and DiFazio, 1988; Yamanoue et al., 1993; Hustveit, 1994).

Descriptions of nonopioid receptor pharmacology, i.e., direct interaction between morphine or fentanyl and human signal transduction proteins, which could be linked to the disparate clinical effects of fentanyl and morphine, are sparse (see NIMH Psychoactive Drug Screening Program database: https://pdsp.unc.edu/databases/pdsp.php). Locus coeruleus (LC) activation may play a role in FIMR and FIRE, and multiple animal studies suggest that fentanyl interacts with α_1-adrenoceptors (Adrs) (Lui et al., 1989, 1990; Tsou et al., 1989; Fu et al., 1997). Additionally fentanyl interacts with the human dopamine transporter in vivo (Bergström et al., 1998) and fentanyl displaces [^{3}H]8-hydroxy-2-(di-n-propylamino)

tetralin (8-OH-DPAT) from serotonin (5-HT) 1A receptors in rat brain preparations (Martin et al., 1991) and transfected cells (Rickli et al., 2018). Finally, fentanyl interacts with the human ether a-go-go–related gene potassium channel, but morphine does not (Katchman et al., 2002; Tschirhart et al., 2019), which could play a role in fentanyl-mediated rapid changes in cardiovascular function.

Data described herein are the first to show that morphine has low affinity (K_i ~100 μM) at the examined recombinant human nonopioid receptors and transporters, whereas fentanyl has high nanomolar or low micromolar K_i or IC_{50} values for displacing radioligand binding or antagonizing function at specific recombinant human α_1-Adr subtypes, the vesicular monoamine transporter (VMAT2), and the dopamine D1 and D4.4 receptor subtypes. Furthermore, carfentanil, a potent fentanyl analog, had binding affinities similar to fentanyl for α_1-Adr subtypes. Conversely, K_i values for fentanyl at displacing radioligand binding at serotonin 1A, 2A, 2B, and 2C; dopamine D2 and D3; cannabinoid CB1; and N-methyl-D-aspartate (NMDA) G2a/G1 receptors as well as at dopamine (DAT), norepinephrine (NET), and serotonin (SERT) transporters were in the high micromolar range. Additionally, we investigated the effects of fentanyl on receptor and transporter function where fentanyl binding affinity was pharmacologically relevant, and the data indicate that fentanyl is an inhibitor/antagonist of function. These data suggest that there are significant differences between morphine and fentanyl pharmacology. This, along with previously published results indicating that the effects

---

ABBREVIATIONS: Adr, adrenoceptor; BSA, bovine serum albumin; CHO, Chinese hamster ovary cells; CNS, central nervous system; DAMGO, [D-Ala^2; N-MePhe^4, Gly-ol]-enkephalin; DAT, dopamine transporter; DHTB, dihydrotetrabenazine; DMEM, Dulbecco's modified Eagle's medium; DPDPE, [D-Pen^2,D-Pen^5]encephalin; DOR, human δ opioid receptor; F/FA, fentanyl and fentanyl analogues; FIMR, fentanyl-induced muscular rigidity; FIRE, fentanyl-induced respiratory effects; GTPγS, guanosine 5′-O-[gamma-thio]triphosphate; 5-HT, serotonin; IP-1, inositol-1 phosphate; HEK, human embryonic kidney cells; K_D, $_{Dissociation\ constant}$; KOR, human κ opioid receptor; LC, locus coeruleus; MK-801 (dizocilpine), (5S,10R)-(+)-5-methyl-10,11-dihydro-5H-dibenzo[a,d]cyclohepten-5,10-imine maleate; MOR, μ opioid receptor; NE, norepinephrine; NET, norepinephrine transporter; NMDA, N-methyl-D-aspartate; 8-OH-DPAT, 8-hydroxy-2-(di-n-propylamino) tetralin; PI, protease inhibitors; RTI-55, methyl (1R,2S,3S)-3-(4-iodophenyl)-8-methyl-8-azabicyclo[3.2.1]octane-2-carboxylate; SCH23390, 7-chloro-3-methyl-1-phenyl-1,2,4,5-tetrahydro-3-benzazepin-8-ol; SERT, serotonin transporter; SKF38393, (±)-1-Phenyl-2,3,4,5-tetrahydro-(1H)-3-benzazepine-7,8-diol; TME buffer 20 mM Tris, 5 mM MgCl2, 1 mM EDTA, pH 7.4 at 4°C U69,593, (+)-(5α,7α,8β)-N-Methyl-N-[7-(1-pyrrolidinyl)-1-oxaspiro[4.5]dec-8-yl]-benzeneacetamide; VMAT2, vesicular monoamine transporter 2.

TABLE 1
Fentanyl and morphine interactions with opioid receptor subtypes
Experiments were conducted as described in the text.

Drug	CHO-rMOR [^{3}H]DAMGO Binding K_i (nM) ± S.E.M. (n) Hill Slope ± S.E.M.	CHO-hKOR [^{3}H]U69,593 Binding K_i (nM) ± S.E.M. (n) Hill Slope ± S.E.M.	CHO-hDOR [^{3}H]DPDPE Binding K_i (nM) ± S.E.M. (n) Hill Slope ± S.E.M.
Fentanyl	0.35 ± 0.05 (16)	125 ± 15 (14)	244 ± 20 (12)
	−0.78 ± 0.05	−0.95 ± 0.04	−1.07 ± 0.04
Morphine	0.58 ± 0.8 (19)	27 ± 3 (15)	178 ± 14 (12)
	−0.97 ± 0.05	−0.98 ± 0.04	−1.06 ± 0.04
	[^{35}S]GTPγS Binding EC$_{50}$ (nM) ± S.E.M. (n) % Max DAMGO Stimulation ± S.E.M.	[^{35}S]GTPγS Binding EC$_{50}$ (nM) ± S.E.M. (n) % Max U69,593 Stimulation ± S.E.M.	[^{35}S]GTPγS Binding EC$_{50}$ (nM) ± S.E.M. (n) % Max DPDPE Stimulation ± S.E.M.
Fentanyl	18 ± 4 (12)	389 ± 41 (14)	1256 ± 153 (13)
	92% ± 4%	85% ± 5%	71% ± 5%
Morphine	38 ± 6 (13)	47 ± 6 (12)	789 ± 92 (13)
	86% ± 3%	94% ± 4%	89% ± 4%

hDOR, human δ opioid receptor; hKOR, human κ opioid receptor; n, number of independent experiments, each conducted with duplicate determinations; rMOR; rat μ opioid receptor.

of F/FAs on animal models of FIMR and FIRE can be blocked with non-MOR antagonists, point to new directions for the development of treatments for the effects of synthetic opioids.

Materials and Methods

Drugs and Chemicals. Fentanyl, carfentanil, morphine, and naloxone were obtained from the Drug Supply Program, National Institute on Drug Abuse (Rockville, MD). Norepinephrine, epinephrine, phenylephrine, prazosin, and tamsulosin were obtained from Sigma-Aldrich Chemical Co. (St. Louis, MO).

[^{3}H] 8-OH-DPAT, [^{3}H]7-chloro-3-methyl-1-phenyl-1,2,4,5-tetrahydro-3-benzazepin-8-ol (SCH23390), [^{125}I]methyl (1R,2S,3S)-3-(4-iodophenyl)-8-methyl-8-azabicyclo [3.2.1]octane-2-carboxylate) (RTI-55), [^{3}H]dopamine, [^{3}H]5HT, [^{3}H]prazosin, [^{3}H]spiperone, [^{3}H]CP-55,940, [^{3}H]MK-801, [^{3}H]dihydrotetrabenazine, and [^{3}H]norepinephrine, were purchased from Perkin Elmer Life and Analytical Sciences (Boston, MA).

All other commonly used reagents were obtained from commercial sources except where specified.

Tissue Culture. Human embryonic kidney cells (HEK-293) or Chinese hamster ovary (CHO) cells were cultured and transfected with the respective recombinant human receptor, rat receptor (MOR), or human transporter by using modifications of previously described methods (Eshleman et al., 1999; Eshleman et al., 2013).

Receptor Binding Assays. Radioligand binding to the VMAT2 (Eshleman et al., 2013; Provencher et al., 2018); dopamine D1, D2, D3, and D4.4 receptors (Eshleman et al., 2013; Janowsky et al., 2014); 5-HT 1A, 2A, 2B, and 2C receptors (Eshleman et al., 2013, 2018); and the dopamine, norepinephrine, and serotonin transporters (Eshleman et al., 1999, 2013) were conducted as previously described. Methods used to examine drug interactions with additional receptors are described below.

α$_1$-Adr Subtypes. To characterize opioid and other drug interactions with the alpha 1 adrenergic receptor subtypes, human embryonic kidney cells expressing the recombinant human α$_{1A}$

adrenergic receptor (HEK-α$_{1A}$-Adr), human α$_{1B}$ adrenergic receptor (HEK-α$_{1B}$-Adr), or the human α$_{1D}$ adrenergic receptor (HEK-α$_{1D}$-Adr) were grown in Dulbecco's modified Eagle's medium (DMEM) supplemented with 10% FetalClone, 300 μg/ml G418, and 0.05% penicillin/streptomycin. The source and plasmid for the receptor cDNAs were Bloomsburg University cDNA Resource Center (Bloomsburg, PA), pcDNA3.1+ (α$_{1A}$-Adr, α$_{1B}$-Adr), and α$_{1D}$-Adr (Genscript, pcDNA3.1+). HEK-293 cells were stably transfected by using modifications of our previously described methods (Shi et al., 2016).

Confluent cells (150-mm plate) were rinsed with PBS, scraped into PBS, and centrifuged for 10 minutes at 1000g and 4°C. The pellet was resuspended and polytronned in Tris buffer (pH 7.4 at 4°C) and centrifuged at 30,000g for 15 minutes at 4°C. The Tris wash was repeated. Cells were resuspended in 3 ml of Tris and stored at −80°C until needed. The binding assay, adapted from published methods (Yang et al., 1998), was performed in duplicate in a 96-well plate. Serial dilutions of test compounds were made by using the Biomek 4000 robotics system (Beckman Coulter, Brea, CA) and assay buffer (50 mM Tris buffer, pH 7.4 at 25°C, containing 0.2 mg/ml ascorbic acid and 100 μM tropolone). The resuspension volumes for each cell line were as follows: α$_{1A}$-Adr, 1 plate/~6.5 ml buffer; α$_{1B}$-Adr, one plate/10 ml buffer; and α$_{1D}$-Adr, two plates/6.5 ml buffer. Membranes were preincubated with drugs for 10 minutes prior to addition of [^{3}H] prazosin (1 to 2 nM final concentration, 80 Ci/mmol; Perkin Elmer) in a final volume of 250 μl. Nonspecific binding was defined with 10 μM phentolamine. The reaction was incubated for 45 minutes at 25°C and terminated by filtration over 0.05% polyethylenimine-soaked "A" filtermats by using cold Tris buffer (50 mM, pH 7.4) with a 6-second wash. Validation compounds included norepinephrine, epinephrine, phenylephrine, prazosin, phentolamine, and tamsulosin. The filters were dried, spotted with scintillation cocktail, and counted for 2 minutes after a 4-hour interval on a Perkin Elmer microbetaplate counter.

Opioid Receptor Subtypes. To characterize drug effects on radioligand binding to human δ and κ opioid receptors (DORs and KORs, respectively) transfected into CHO cells (provided by SRI) and rat MOR transfected into CHO cells (provided by Dr. Thomas Murray), cell lines were maintained in DMEM supplemented with 10% FBS,

TABLE 2
[^{3}H]Prazosin saturation binding to HEK-α$_{1A}$-Adr, HEK-α$_{1B}$-Adr, and HEK-α$_{1D}$-Adr receptor subtypes: [^{3}H]Prazosin K$_D$ and B_{max} values
[^{3}H]Prazosin was tested at concentrations ranging from 0.08 to 2.5 nM. Assays were conducted in duplicate. Experiments were conducted as described in the text.

Receptor	[^{3}H]Prazosin Binding B_{max} (pmol/mg) ± S.E.M. (n)	K$_D$ (nM) ± S.E.M.
α$_{1A}$-Adr	6.39 ± 0.30 (3)	0.153 ± 0.052
α$_{1B}$-Adr	7.7 ± 1.7 (3)	0.147 ± 0.018
α$_{1D}$-Adr	1.12 ± 0.18 (3)	0.186 ± 0.003

n, number of independent experiments, each conducted with duplicate determinations.
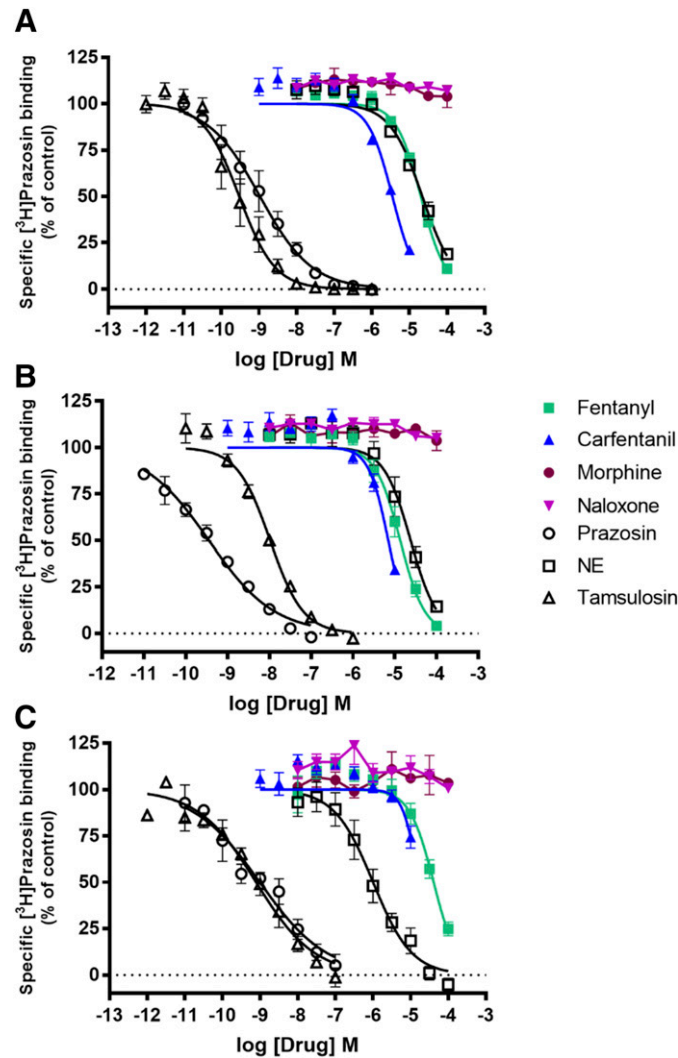
Fig. 2. Displacement of specific [^{3}H]Prazosin binding by opioids and antagonists at α_{1A}-Adr (A), α_{1B}-Adr (B), and α_{1D}-Adr (C) receptor subtypes. Data shown are the means $\pm$ S.E.M. of three to five experiments, except if a drug had no effect when $n = 2$.

400 µg/ml G418, and 0.1% penicillin/streptomycin. All cell lines were grown to confluence and then harvested for membrane preparation. The membranes for binding assays were prepared in 50 mM of Tris buffer (pH 7.5 at 4°C). Cells were scraped from the plates in calcium/magnesium free-PBS and centrifuged at 500g for 15 minutes. The cell pellet was homogenized in 2 ml buffer with a polytron, diluted with 11 ml buffer, and centrifuged at 40,000g for 15 minutes; then it was washed and recentrifuged. The final pellet was covered with 3 ml buffer and stored at −80°C until needed.

Binding assays were conducted by using [^{3}H][D-Ala^2, N-MePhe^4, Gly-ol]-enkephalin (DAMGO), [^{3}H] [D-Pen^2,D-Pen^5]encephalin (DPDPE) (0.8 nM, ~20,000 cpm), and [^{3}H](+)-(5α,7α,8β)-N-Methyl-N-[7-(1-pyrrolidinyl)-1-oxaspiro[4.5]dec-8-yl]-benzeneacetamide (U69,593) (0.8 nM, ~22,000 cpm) at the MORs, DORs, and KORs, respectively. The assays were performed in duplicate in 96-well plates by using 50 mM Tris buffer (pH 7.7 at room temperature). Nonspecific binding was determined with 1.0 µM of the unlabeled analog of each radioligand. Cell membranes were incubated with the appropriate radioligand and test compound at 25°C for 60 minutes. The incubation was terminated by rapid filtration through Perkin Elmer Filtermat A filters presoaked in 0.05% polyethylenimine on a Tomtec cell harvester, and bound radioactivity was determined as described for other receptors above. For [^{3}H]DAMGO, [^{3}H]DPDPE, and [^{3}H]U69,593, the dissociation constant K$_D$ values are 0.147, 0.789, and 0.65 nM,

respectively. The densities of receptors are 0.373 $\pm$ 0.095, 32.8 $\pm$ 1.7, and 11.29 $\pm$ 0.34 pmol/mg protein for the MOR, DOR, and KOR cell lines, respectively.

CB1 Cannabinoid Receptor. The method for [^{3}H]CP-55,940 binding assays was adapted from Farrens et al. (2002). The source and plasmid for the receptor cDNA was cDNA Resource Center and pcDNA3.1+. HEK-293 cells were transfected by using lipofectamine 2000 (Invitrogen). WIN 55,212 (10 µM) was used to define nonspecific binding. HEK-CB1 cells were grown until confluent on 15-cm dishes. Cells were scraped into 7 ml of calcium/magnesium free-PBS and centrifuged at 11,000g for 10 minutes. The supernatant was decanted, and the pellet was resuspended with a Polytron in 5 ml of hypotonic buffer [5 mM Tris, 2 mM EDTA + protease inhibitors (PI)]. The homogenate was centrifuged at 35,000g for 20 minutes and resuspended in TME buffer (20 mM Tris, 5 mM MgCl2, 1 mM EDTA, pH 7.4 at 4°C with PI) by using a Polytron. After centrifugation at 35,000g for 20 minutes, the pellet was resuspended in TME + PI buffer (1.6–3 ml for competition or saturation binding assay) by using a Polytron. Proteins were quantified by using the BCA kit (Thermo Fisher, Waltham, MA).

Binding assays used TME supplemented with 5 mg bovine serum albumin (BSA)/ml, pH 7.4, at 30°C. The reaction included test compounds or WIN-55,212, membrane preparation (15–70 µg, depending on the expression level of CB1), [^{3}H]CP-55,940, and TME

TABLE 3

HEK-α_{1A}-Adr, HEK-α_{1B}-Adr, and HEK-α_{1D}-Adr: effects of fentanyl, carfentanil, morphine, naloxone, and Adr1 agonists and antagonists on [^{3}H]prazosin binding and IP-1 formation

For each receptor, standard agonists and antagonists were tested: Adr1 agonists NE, epinephrine (EPI), and phenylephrine and Adr1 antagonists prazosin and tamulosin.

Drug	[^{3}H]Prazosin Binding			Drug-Stimulated IP-1 Accumulation			Inhibition of NE-Stimulated IP-1 Accumulation		
	K_i (nM) ± S.E.M. (n) Hill Slope ±S.E.M.			EC_{50} (nM) ± S.E.M. (n) % Max NE ± S.E.M.[a]			IC_{50} (nM) ± S.E.M. (n) % Max Inhibition ± S.E.M.[b]		
	α_{1A}-Adr	α_{1B}-Adr	α_{1D}-Adr	α_{1A}-Adr	α_{1B}-Adr	Adr1D	α_{1A}-Adr	α_{1B}-Adr	α_{1D}-Adr
Fentanyl	1407 ± 81 (5) −1.32 ± 0.05	1100 ± 250 (3) −1.51 ± 0.08	4110 ± 450 (4) −1.41 ± 0.21	>100 μM (2) 0%	>100 μM (2) <1%	>20 μM (6) 3.5 ± 2.5%	3660 ± 790 (3) 100%	3690 ± 300 (3) 100%	11,900 ± 1600 (3) 73 ± 13%
Carfentanil	418 ± 24 −1.35 ± 0.04	828 ± 57 −1.93 ± 0.31	2490 ± 530 −1.54 ± 0.11	>10 μM (5) 0%	>10 μM (2) 0%	>10 μM (2) 0%	2040 ± 380 (6) 100%	1030 ± 150 (6) 99.9 ± 0.1%	>10 μM (3) 5.7 ± 2.6%
Morphine	>100 μM (2) ND	>100 μM (2) ND	>100 μM (2) ND	>100 μM (2) 0%	>100 μM (2) <3%	>100 μM (4) 0%	>100 μM (2) 16.3% ± 3.7%	>100 μM (2) <7%	>100 μM (2) <5%
Naloxone	>100 μM (2) ND	>100 μM (2) ND	>100 μM (2) ND						
Norepinephrine	1580 ± 220 (5) −1.01 ± 0.04	1920 ± 490 (3) −1.45 ± 0.20	131 ± 40 (5) −0.94 ± 0.15	55 ± 12 (3) 102.8% ± 3.3%	39.7 ± 5.8 (3) 104.1% ± 3.6%	37.0 ± 5.8 (3) 95.89% ± 0.63%			
Epinephrine	730 ± 140 (3) −1.05 ± 0.07	790 ± 150 (3) −1.23 ± 0.05	185 ± 22 (3) −1.06 ± 0.03	22.7 ± 5.0 (4) 106.1% ± 1.4%	10.0 ± 2.3 (3) 100.6% ± 4.6%	32.1 ± 9.8 (3) 103.0% ± 4.6%			
Phenylephrine	4880 ± 410 (5) −1.26 ± 0.09	4900 ± 1100 (3) −1.92 ± 0.39	1850 ± 230 (3) −1.11 ± 0.05	318 ± 13 (3) 106.3% ± 1.6%	330 ± 110 (4) 95.3% ± 5.9%	620 ± 140 (4) 70.1% ± 1.2%			
Prazosin	0.134 ± 0.057 (3) −0.72 ± 0.09	0.027 ± 0.008 (8) −0.56 ± 0.04	0.115 ± 0.037 (4) −0.51 ± 0.09				4.02 ± 0.54 (3) 100%	8.7 ± 2.7 (5) 100%	0.48 ± 0.12 (3) 99.06% ± 0.77%
Tamsulosin	0.038 ± 0.013 (3) −0.96 ± 0.05	0.769 ± 0.043 (3) −1.05 ± 0.05	0.084 ± 0.023 (3) −0.56 ± 0.07				1.95 ± 0.85 (4) 100%	5.04 ± 0.44 (4) 100%	0.339 ± 0.061 (4) 100%

n, number of independent experiments, each conducted with duplicate determinations; ND, not determined.
[a]Maximal agonist effects were normalized to the maximal stimulation by 10 μM norepinephrine.
[b]Maximal antagonist effects were normalized to the maximal inhibition by 100 nM tamsulosin.
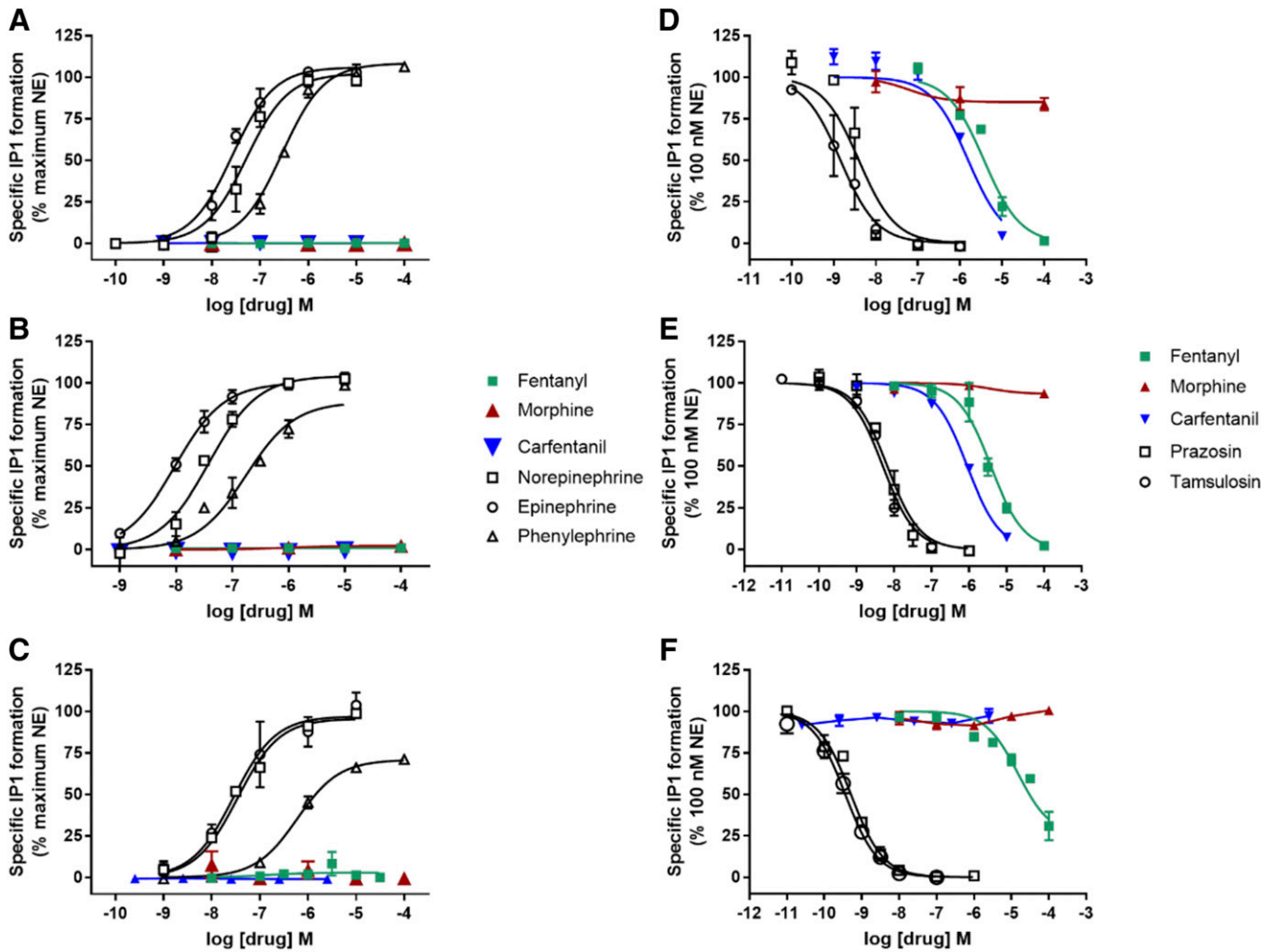
Fig. 3. HEK-α_{1A}-Adr, HEK-α_{1B}-Adr, and HEK-α_{1D}-Adr: IP-1 agonist and antagonist dose-response curves. Agonist stimulation of IP-1 formation of α_{1A}-Adr (A), α_{1B}-Adr 1B (B), and (C) α_{1D}-Adr receptor subtypes. Antagonist inhibition of norepinephrine-stimulated IP-1 formation of α_{1A}-Adr (D), α_{1B}-Adr (E), and α_{1D}-Adr (F) receptor subtypes. Data shown are the means ± S.E.M. of three to six experiments, except if a drug had no effect when $n = 2$.

+ BSA buffer to a final volume of 0.5 ml. In saturation binding assays, the range of concentrations of [^{3}H]CP-55,940 was 0.07–3 nM. In competition binding assays, the concentration of [^{3}H]CP-55,940 was 1.2–1.5 nM. After incubation at 30°C for 60 minutes, the reaction was terminated by filtration with TME + 1 mg BSA/ml over Filtermat A filters presoaked in 0.2% polyethylenimine. An additional wash was added to the normal harvesting program to reduce nonspecific binding.

NMDA Receptor Binding. The methods were adapted from Grant et al. (1997). For functional NMDA receptors, cells need to express two NMDA receptor subunits, the GluN1a and the GluN2a. However, simultaneous and stable expression of both subunits is toxic to the cell (Grant et al., 1997; unpublished results). We developed a method by using a cell line that stably expresses one of the subunits (GluN2a) and is subsequently transfected with the cDNA for the other subunit (GluN1a) the week of the experiment.

HEK cells stably expressing the GluN2a subunit (G2a-Myc cDNA; Origene) were transfected with 10 μg of Grin1-tGFP cDNA (Origene), using the polyethylenimine as we have previously described (Shi et al., 2016). On day 2, medium was changed to DMEM supplemented with selection antibiotic G418 (300 μg/ml). To reduce coexpression toxicity, the receptors were blocked with 100 μM of ketamine (adapted from Grant et al., 1997) and incubated for 48 hours. On day 4, cells were harvested by pouring off the medium and rinsing with 10 ml of HEPES buffer (20 mM), and each plate of cells was scraped into 10 ml of high

Mg2+ buffer (20 mM HEPES, 100 μM glycine, 100 μM glutamate, 300 μM MgCl2, pH 7.5). To remove the ketamine, cells were incubated for 30 minutes at 32°C and centrifuged for 10 minutes at 48,000g at 4°C. EDTA buffer (20 mM HEPES, 1 mM EDTA, pH 7.5) was added, the pellet was homogenized by using a Polytron, and the membranes were incubated for 30 minutes at 32°C. After centrifugation, the pellet was polytronned in ~3 ml assay buffer (20 mM HEPES, 100 μM glycine, 100 μM glutamate, 100 μM MgCl2, 0.2 mg/ml ascorbic acid, pH 7.5).

The binding assay included drug, membrane preparation, [^{3}H]MK-801 (~20 nM), and assay buffer in a final volume of 250 μl. Specific binding was defined as the difference between total binding and nonspecific binding in the presence of 10 μM unlabeled MK-801. The reaction was incubated for 60 minutes at 22°C and was terminated by filtration with 20 mM of ice-cold HEPES buffer, pH 7.5, through Perkin Elmer A filtermats presoaked in 0.5% polyethylenimine, using a Tomtec 96-well harvester. Radioactivity remaining on filters was counted in a Perkin Elmer microbetaplate reader.

Assays of Function. Assays of VMAT2 function (Eshleman et al., 2013; Provencher et al., 2018), dopamine D1 and D4.4 receptor function (Eshleman et al., 2013; Janowsky et al., 2014), and [^{3}H] neurotransmitter uptake by the dopamine, norepinephrine, and serotonin transporters (Eshleman et al., 1999, 2013) were conducted as we have previously described in detail. Methods used to examine drug effects on other receptor-mediated signal transduction pathways are described below.

TABLE 4
K_i values for inhibition of radioligand binding to and IC_{50} values for inhibition of [³H]neurotransmitter uptake by HEK-hDAT, HEK-hSERT, HEK-hNET, and HEK-hVMAT2 cells
For each transporter, METH was tested as a standard substrate. For VMAT2, DHTB was tested as the standard blocker. For DAT, SERT, and NET, cocaine was tested as the standard blocker.

Drug	hDAT [125I]RTI-55 Binding K_i (nM) ± S.E.M. Hill Slope ±S.E.M. (n)	hDAT [³H]DA Uptake IC_{50} (nM) ± S.E.M. (n)	hSERT [125I]RTI-55 Binding K_i (nM) ± S.E.M. Hill Slope ±S.E.M. (n)	hSERT [³H]5-HT Uptake IC_{50} (nM) ± S.E.M. (n)	hNET [125I]RTI-55 Binding K_i (nM) ± S.E.M. Hill Slope ±S.E.M. (n)	hNET [³H]NE Uptake IC_{50} (nM) ± S.E.M. (n)	hVMAT2 [³H]DHTB Binding K_i (nM) ± S.E.M. Hill Slope ±S.E.M. (n)	hVMAT [³H]5-HT Uptake IC_{50} (nM) ± S.E.M. (n)
Fentanyl	40,270 ± 2400 −1.17 ± 0.19 (3)	29,700 ± 7700 (4)	69,000 ± 15,000 −1.20 ± 0.06 (5)	>85,000 (3)	13,000 ± 2800 −1.42 ± 0.40 (3)	27,500 ± 6700 (4)	56,100 ± 2700 −1.48 ± 0.09 (3)	911 ± 34 (4)
Carfentanil	>10,000 (3)	>20,000 (4)	>10,000 (3)	>20,000 (3)	>10,000 (3)	4460 ± 870 (3)	>10,000 (3)	4100 ± 1100 (3)
Morphine	>99 μM ND (3)	>100 μM (2)	>78 μM ND (3)	>83,000 (3)	>90,000 ND (5)	>100 μM (2)	>100 μM (3) ND	>100 μM (2)
Cocaine	554 ± 60 −1.12 ± 0.09 (4)	278 ± 32 (5)	404.4 ± 6.8 −1.06 ± 0.08 (3)	260 ± 100 (3)	1550 ± 250 −1.48 ± 0.30 (3)	303 ± 54 (5)		
METH	2760 ± 660 −1.38 ± 0.04 (3)	62.6 ± 2.2 (3)	117,000 ± 14,000 −1.23 ± 0.16 (3)	5800 ± 470 (3)	1630 ± 180 −1.12 ± 0.04 (5)	12.1 ± 1.2 (4)	684,000 ± 65,000 −1.01 ± 0.07 (3)	4180 ± 600 (4)
DHTB							74 ± 28 −1.28 ± 0.13 (3)	41.5 ± 3.3 (5)

METH, methamphetamine; ND, Hill slope was not determined because of the low affinity of the compound; n, number of independent experiments, each conducted with duplicate determinations.

α_1-Adr–Mediated Inositol-1-Phosphate Formation. HEK-α_{1A}-Adr, HEK-α_{1B}-Adr, or HEK-α_{1D}-Adr cells were used for assays involving the IP-One Gq ELISA kit (CisBio, Bedford, MA). The methods are an adaptation of our 5HT2A inositol-1-phosphate (IP-1) assay (Eshleman et al., 2013). The day before an experiment, cells were plated in 24-well plates at a density of 400,000 cells/well by using DMEM supplemented with charcoal-stripped FetalClone and penicillin/streptomycin. For HEK-α_{1A}-Adr cells, on the day of the experiment, medium was removed and cells were preincubated with 1 ml of unsupplemented medium for 1 hour. HEK-α_{1B}-Adr or HEK-α_{1D}-Adr cells were used without rinsing. Drugs were made up in stimulation buffer supplied in the kit supplemented with 100 μM of tropolone. Medium was removed from the well, antagonist or buffer was added, and cells were preincubated for 10 minutes. Agonists were added, cells were incubated for 1 hour and lysed for 30 minutes, and 50 μl of cell lysate was added to the IP-1 plates. After the addition of appropriate antibodies, plates were incubated overnight at 4°C, washed six times, and incubated with substrate for 20 minutes, and after termination of the reaction, the plate was read on a plate reader at 450 nm with a correction at 620 nm. Agonist effects were normalized to the maximal stimulation by norepinephrine, and antagonists were tested in the presence of 100 nM norepinephrine and normalized to the inhibition by 100 nM tamsulosin.

Opioid (δ and κ) Receptor–Mediated [³⁵S]GTPγS Binding. The membranes for [³⁵S]GTPγS binding assays were prepared in 20 mM of HEPES, 10 mM of MgCl₂, 100 mM of NaCl, and 0.2 mM of dithiothreitol (pH 7.4). Cells were scraped from the plates and centrifuged at 500*g* for 15 minutes. The resulting pellet was homogenized in 2 ml of buffer with a polytron, diluted with 11 ml of buffer, centrifuged at 40,000*g* for 15 minutes, and washed and recentrifuged. The final pellet was covered with 3 ml of buffer and stored at −80°C until needed. The membranes were incubated with [³⁵S]GTPγS (50 pM), GDP (10 μM), and the test compound in a total volume of 1 ml for 60 minutes at 25°C (Traynor and Nahorski, 1995). Samples were filtered over Perkin Elmer FiltermatA filters and counted as described for the binding assays. A dose response curve with a prototypical full agonist (DPDPE and U69,593 for DORs and KORs, respectively) was conducted in each experiment to identify full and partial agonists.

Opioid (μ) Receptor-Mediated [³⁵S]GTPγS Binding. Comparisons of morphine-like and synthetic opioids on β-arrestin 2 have been well described (de Waal et al., 2020; Vasudevan et al., 2020). Fentanyl and related analogs, as well as morphine-like compounds, exert effects via a β-arrestin 2–mediated pathway that is hypothesized to play a role in the unwanted side effects of opioids. Here, we executed a head-to-head comparison of the effects of morphine and fentanyl on opioid receptor–mediated $G\alpha_{i/o}$ activation as well as effects on nonopioid receptor function. Membranes were prepared in 20 mM of HEPES, 10 mM of MgCl₂, 100 mM of NaCl, 1 mM of EDTA, and 0.2 mM of dithiothreitol (pH 7.4). Cells were starved for 12–18 hours prior to harvest in unsupplemented DMEM. Cells were scraped from the plates and centrifuged at 500*g* for 15 minutes. The cell pellet was homogenized in 2 ml of buffer with a polytron, diluted with 11 ml of buffer, centrifuged at 40,000*g* for 15 minutes, and washed and recentrifuged. The final pellet was overlaid with 3 ml of buffer and stored at −80°C until use. For agonist assays, the membrane was incubated with [³⁵S]GTPγS (50 pM), GDP (1 μM), and the test compound in a total volume of 1 ml for 60 minutes at 25°C. Samples were filtered over glass fiber filters and washed with ice-cold saline. A dose-response curve with DAMGO was conducted in each agonist experiment to identify full and partial agonist compounds.

Data Analysis. Sigmoidal curves resulting in IC_{50} values for displacement of radioligand or inhibition of second messenger generation were analyzed by using a nonlinear curve-fitting program and further analyzed by using unpaired *t* tests or one-way ANOVAs followed by either Dunnett's or Tukey's multiple comparisons test (Prism version 7; GraphPad Software, La Jolla, CA). Saturation binding data were analyzed by nonlinear regression to generate K_D
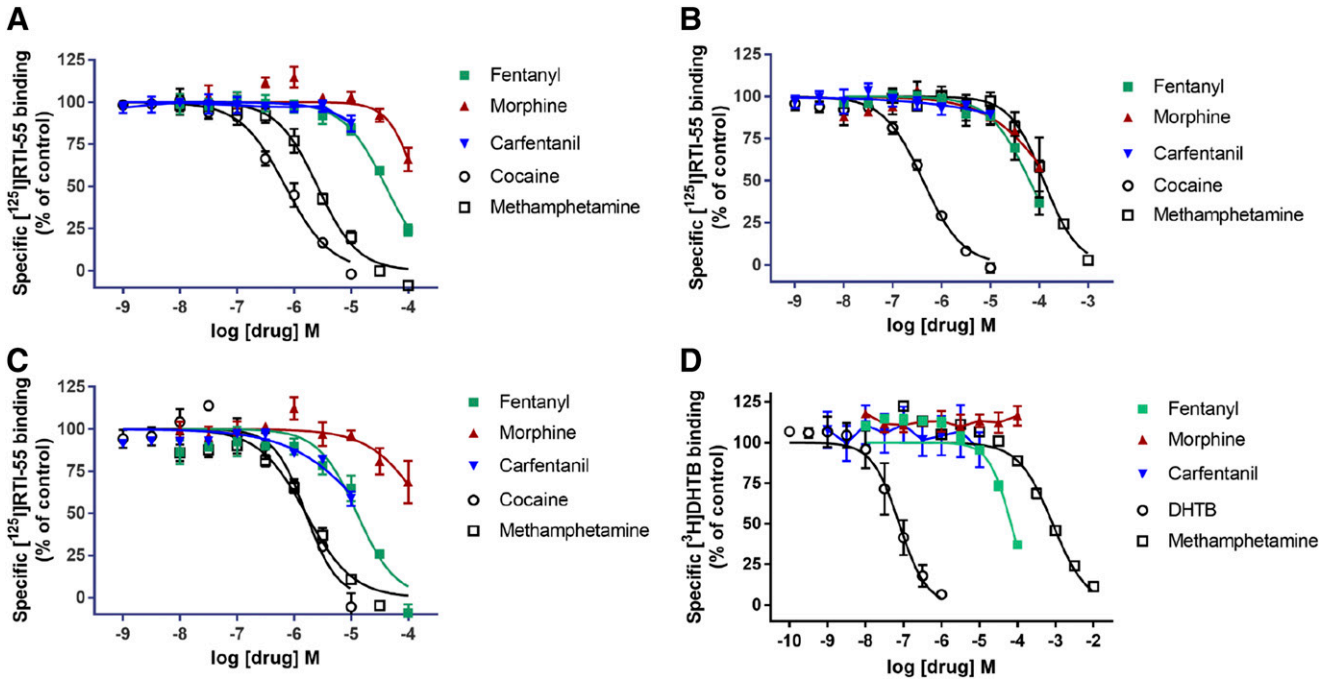
Fig. 4. Opioid effects on radioligand binding to transporters. ([^{125}I]RTI-55) binding to HEK-hDAT (A), hSERT (B), and hNET (C). (D) [^{3}H]DHTB binding to hVMAT2. Data shown are the means $\pm$ S.E.M. of three to five experiments, except if a drug had no effect when $n = 2$.

and B_{max} values as we have previously described (Eshleman et al., 2013, 2018; Janowsky et al., 2014).

Results

Fentanyl and Morphine Interactions with Opioid Receptor Subtypes. Fentanyl and morphine (Fig. 1) had highest affinity for MOR ([^{3}H]DAMGO binding), as compared

with their affinities for KOR and DOR subtypes, and the rank order of affinities across receptors were similar ($\mu >> \kappa > \delta$) (Table 1). However, fentanyl had higher selectivity, i.e., its affinities for KOR (357-fold) and DOR (697-fold) were much lower than its affinity for the MOR compared with morphine, which differed less in affinities for the KORs (46-fold) and DORs (306-fold). In assays of receptor function ([^{35}S]GTPγS binding), potency differences paralleled affinity differences in
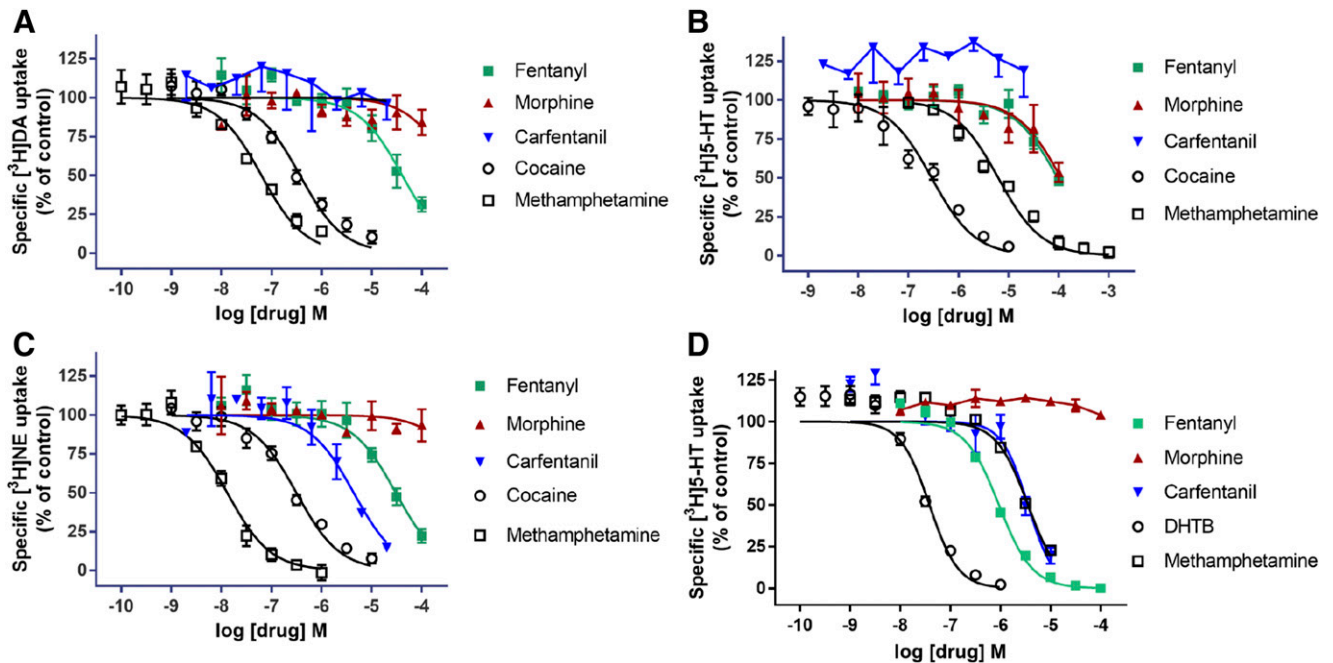

Fig. 5. Opioid effects on [^{3}H]neurotransmitter uptake by HEK-hDAT, -hSERT, -hNET, and -hVMAT2. (A) hDAT ([^{3}H] dopamine); (B) hSERT ([^{3}H] 5-HT); (C) hNET ([^{3}H] NE); (D) hVMAT2 ([^{3}H] 5-HT). Data shown are the means $\pm$ S.E.M. of three to five experiments, except if a drug had no effect when $n = 2$.

TABLE 5
Drug effects on radioligand binding to dopamine D1, D2, D3, and D4.4 receptors
For each receptor, a standard agonist (SKF38393 or quinpirole) and antagonist (SCH23390, butaclamol, or haloperidol) was tested.

Drug	DA D1R [³H]SCH 23390 K_i (nM) ± S.E.M. (n) Hill Slope ±S.E.M.	DA D2R [³H]Spiperone K_i (nM) ± S.E.M. (n) Hill Slope ±S.E.M.	DA D3R [³H]Spiperone K_i (nM) ± S.E.M. (n) Hill Slope ±S.E.M.	DA D4.4R [³H]Spiperone K_i (nM) ± S.E.M. (n) Hill Slope ±S.E.M.
Fentanyl	1670 ± 200 (3) −1.17 ± 0.07	14,900 ± 1800 (3) −1.20 ± 0.06	12,100 ± 910 (5) −0.88 ± 0.11	1049 ± 74 (3) −1.13 ± 0.02
Morphine	>100 μM (3) ND	>100 μM (3) ND	>100 μM (3) ND	>100 μM (3) ND
SKF38393	79 ± 12 (3) −1.03 ± 0.04			
SCH23390	0.159 ± 0.018 (3) −1.16 ± 0.03			
Quinpirole		15,700 ± 4900 (6) −0.79 ± 0.08	130 ± 20 (6) −0.73 ± 0.03	157.4 ± 7.8 (3) −0.80 ± 0.01
Butaclamol		0.58 ± 0.13 (7) −0.83 ± 0.18	8.2 ± 3.5 (6) −1.15 ± 0.30	
Haloperidol				4.60 ± 0.27 (3) −0.98 ± 0.01

n, number of independent experiments, each conducted with duplicate determinations; ND, not determined.

terms of selectivity. Fentanyl was an apparent full agonist at the MOR but, under the assay conditions described here, was a partial agonist at DOR (71% efficacy compared with DPDPE, $P < 0.0001$, one-way ANOVA followed by Dunnett's multiple comparison test) and KOR (85% compared with U50,488H, $P < 0.05$). Morphine, however, was a full agonist at KOR but a partial agonist at DOR ($P < 0.05$) and MOR ($P < 0.01$) (Table 1).

Fentanyl, Carfentanil, Morphine, and Naloxone Interactions with α_1-Adr Subtypes. In initial experiments, equilibrium saturation binding of [³H]prazosin to recombinant human α_{1A}-Adr, α_{1B}-Adr, and α_{1D}-Adr subtypes stably expressed in HEK293 cells was characterized, and K_D and B_{max} values were determined (Table 2). For α_{1A}-Adr, the [³H]prazosin K_D was 0.153 ± 0.052 nM and the B_{max} was 6.39 ± 0.3 pmol/mg protein. For α_{1B}-Adr, the K_D was 0.147 ± 0.018 nM and the B_{max} was 7.7 ± 1.7 pmol/mg protein. For α_{1D}-Adr, the K_D was 0.186 ± 0.003 nM and the B_{max} was 1.12 ± 0.18 pmol/mg protein. Thus, the K_D values across receptor subtypes were in the high picomolar range but differed significantly (one-way ANOVA followed by Tukey's multiple comparison test, $P < 0.05$). These K_D values were used to
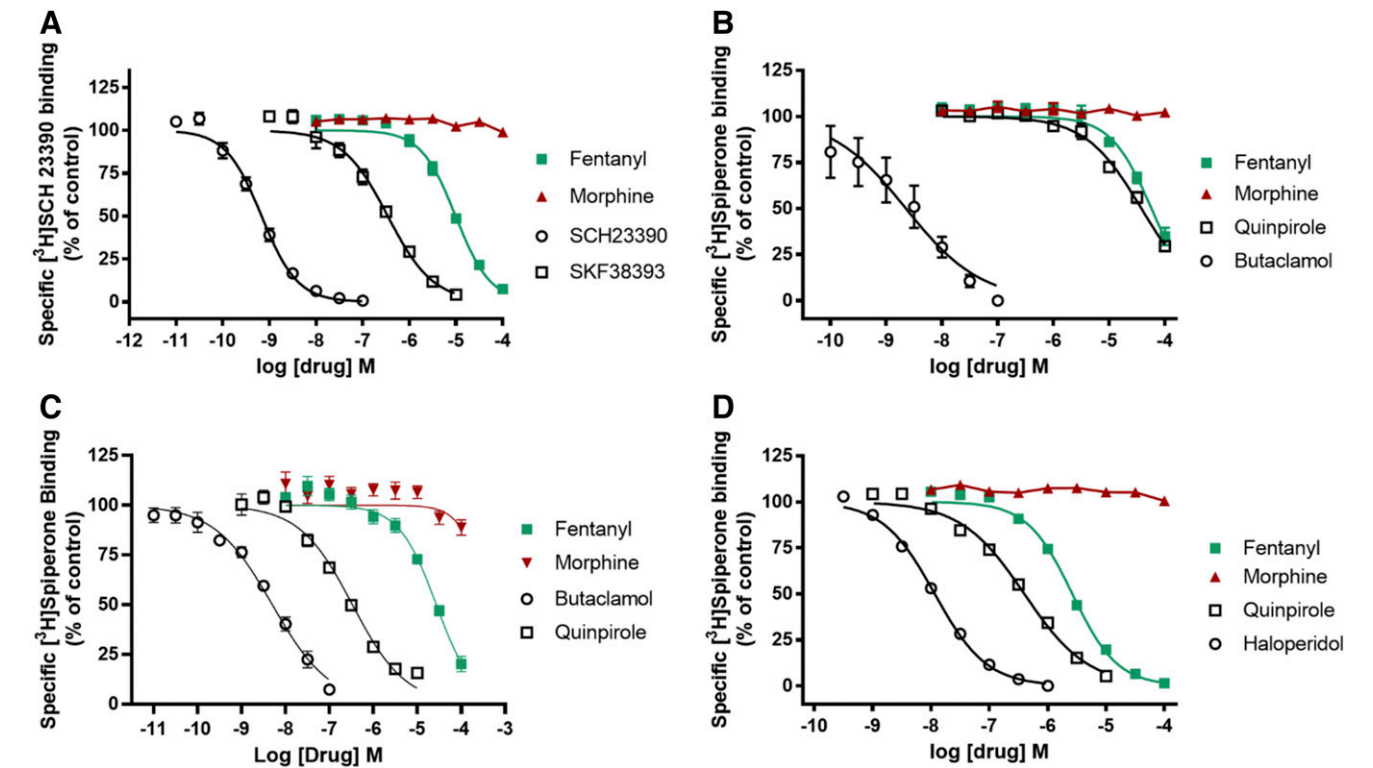

Fig. 6. Drug effects on radioligand binding to dopamine D1, D2, D3, and D4.4 receptors. (A) Dopamine D1 receptor ([³H]SCH 23390); (B) dopamine D2 receptor ([³H]spiperone); (C) dopamine D3 receptor ([³H]spiperone); and (D) dopamine D4.4 receptor ([³H]spiperone). Data shown are the means ± S.E.M. of three to seven experiments.

TABLE 6
Effects of fentanyl and morphine on recombinant human dopamine D1 and D4.4 receptor function

Assays were run in duplicate with six to seven concentrations of the test compound. The standard agonist dopamine was tested in the agonist experiments, and the antagonists SCH23390 (D1) or haloperidol (D4.4) were tested in the antagonist experiment.

Drug (Agonists)	C6-D1 EC_{50} (nM) ± S.E.M. (n) % Max Dopamine ±S.E.M.	C6-D1 IC_{50} (nM) ± S.E.M. (n) % Max Inhibition of 100 nM Dihydrexidine ± S.E.M.	HEK-D4.4-AC1 EC_{50} (nM) ± S.E.M. (n) % Max Quinpirole ± S.E.M.	HEK-D4.4-AC1 IC_{50} (nM) ± S.E.M. (n) % Max Reversal of 100 nM Quinpirole ±S.E.M.
Fentanyl	>100 μM (2)	27,000 ± 5500 (5)	>50 μM (6) (three of six curves could be fit)	12,700 ± 2500 (4)
	0%	65.5% ± 4.0%	36% ± 11%	63% ± 20%
Morphine	>100 μM (2)	>100 μM (2)	>40 μM (5) (three of five curves could be fit)	>100 μM (3)
	13% ± 13%	4.5% ± 4.5%	20% ± 11%	Minimal effect
Dopamine	19.5 ± 1.7		4.4 ± 1.5 (4)	
	91.6% ± 5.9%		95.1% ± 1.8%	
Quinpirole			0.60 ± 0.25 (6)	
			95.4 ± 3.9%	
SCH23390		3.90 ± 0.52 (4)		
		98.36% ± 0.26%		
Haloperidol				152 ± 55 (4)
				117% ± 26%

n, number of independent experiments, each conducted with duplicate determinations.

calculate K_i values in subsequent experiments that examined drug-receptor interactions (Cheng and Prusoff, 1973).

Fentanyl had K_i values in the low micromolar range at each receptor subtype, with a rank order of affinity of α_{1B}-Adr ≥ α_{1A}-Adr > α_{1D}-Adr (P < 0.001, one-way ANOVA followed by Tukey's multiple comparison, Fig. 2; Table 3). Carfentanil similarly demonstrated K_i values in the low micromolar range with a rank order of affinity of α_{1A}-Adr > α_{1B}-Adr > α_{1D}-Adr. In contrast, K_i values for morphine and naloxone at each receptor subtype were greater than 100 μM. Norepinephrine,

epinephrine, and phenylephrine displaced [^{3}H]prazosin binding with rank orders of affinity of α_{1D}-Adr >> α_{1A}-Adr ≥ α_{1B}-Adr (Table 3, P < 0.01, one-way ANOVA followed by Tukey's multiple comparison). Importantly, fentanyl and norepinephrine, the endogenous agonist, had similar affinities for α_{1A}-Adr and α_{1B}-Adr (P > 0.05, one-way ANOVA followed by Dunnett's multiple comparison), whereas carfentanil had a ~threefold higher affinity at α_{1A}-Adr. Carfentanil had higher affinity than norepinephrine at α_{1B}-Adr, but both fentanyl and carfentanil had much lower affinity than norepinephrine at
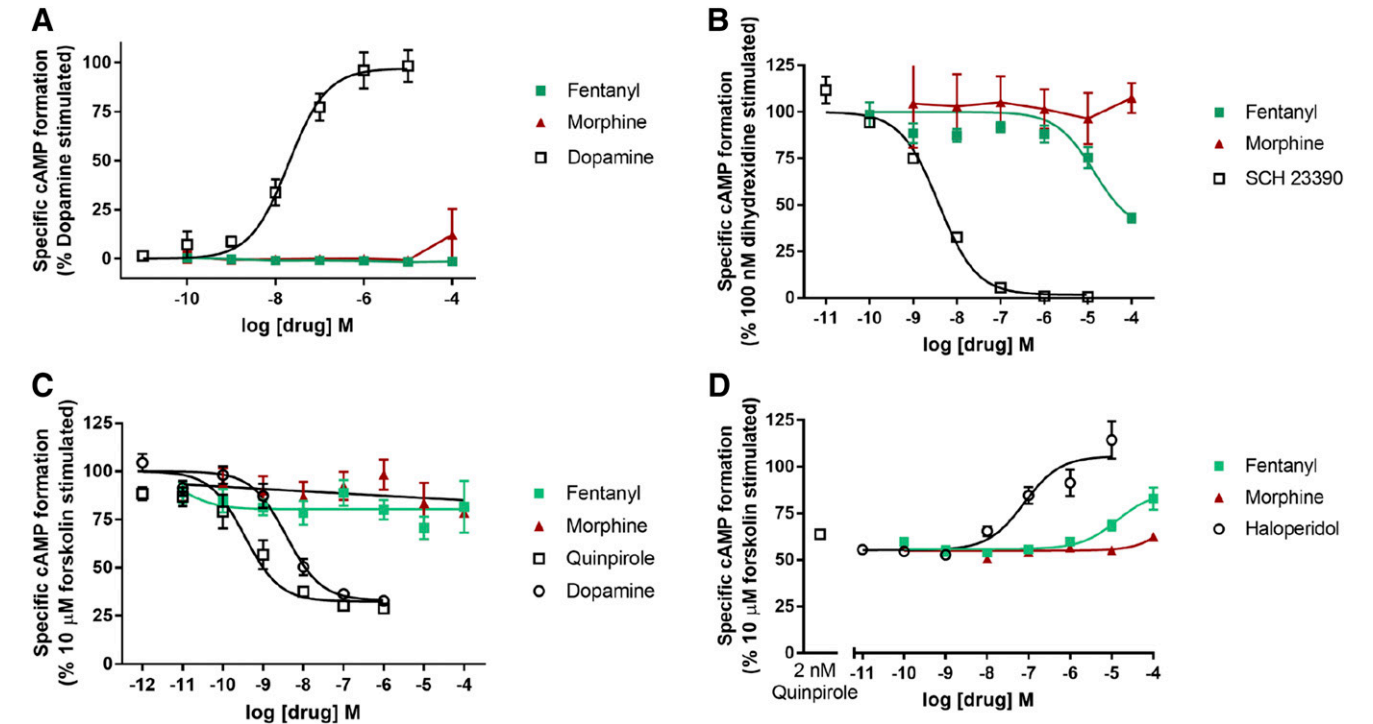

Fig. 7. Agonist, antagonist, and opioid effects on dopamine D1 and D4.4 receptor–mediated adenylyl cyclase. (A) D1 agonist stimulation of adenylyl cyclase. (B) D1 antagonist inhibition of 100 nM dihydrexidine-stimulated adenylyl cyclase activity. (C) D4.4 agonist inhibition of 10 μM forskolin-stimulated adenylyl cyclase. (D) D4.4 antagonist reversal of 2 nM quinpirole inhibition of forskolin-stimulated adenylyl cyclase. Data shown are the means ± S.E.M. of three to six experiments.

TABLE 7

Displacement of [^{3}H]radioligand from recombinant human serotonin 5HT1A, 5HT2A, 5HT2B, and 5HT2C as well as cannabinoid CB1 and glutamate NMDA (G2a/G1) receptors

For each serotonin receptor subtype, the standard agonist 5-HT and a selective antagonist (WAY 100635, ketanserin, SB204741, or SB242084) were tested. For the CB1 receptor, the standard agonists WIN 55,212 and THC were tested. For the NMDA receptor, the standard antagonists MK-801 and phencyclidine were tested.

Drug	5HT1A [^{3}H]8-OH-DPAT Binding K_i (nM) ± S.E.M. (n) Hill Slope ±S.E.M.	5HT2A [^{3}H]5-HT Binding K_i (nM) ± S.E.M. (n) Hill Slope ±S.E.M.	5HT2B [^{3}H]5-HT Binding K_i (nM) ± S.E.M. (n) Hill Slope ±S.E.M.	5HT2C [^{3}H]5-HT Binding K_i (nM) ± S.E.M. (n) Hill Slope ±S.E.M.	CB1 [^{3}H]CP,940 Binding K_i (nM) ± S.E.M. (n) Hill Slope ±S.E.M.	NMDA (G2a/G1) [^{3}H]MK-801 Binding K_i (nM) ± S.E.M. Hill Slope ±S.E.M.
Fentanyl	2240 ± 240 (3) −1.06 ± 0.03	31,400 ± 3000 (3) −1.02 ± 0.03	8600 ± 1200 (3) −0.87 ± 0.09	114,000 ± 23,000 (3) −0.89 ± 0.02	>100 µM (2)	>52 µM (4)
Morphine	>100 µM (3) ND	>100 µM (3) ND	>100 µM (3) ND	>100 µM (3) ND	>100 µM (2)	>100 µM (2)
5-HT	5.89 ± 0.71 (3) −0.90 ± 0.06	26.77 ± 0.56 (3) −1.03 ± 0.10	3.24 ± 0.11 (3) −0.87 ± 0.03	6.46 ± 0.77 (3) −0.96 ± 0.03		
WAY 100635	0.60 ± 0.33 (7) −1.27 ± 0.22					
Ketanserin		13.1 ± 1.3 (3) −0.43 ± 0.04				
SB204741			52 ± 14 (3) −0.63 ± 0.06			
SB242084				2.87 ± 0.67 −1.17 ± 0.16		
WIN 55,212					244 ± 78 (3) −0.80 ± 0.06	
THC					30 ± 10 (5) −0.82 ± 0.18	
MK-801						17.3 ± 1.6 (5) −0.80 ± 0.06
Phencyclidine						2870 ± 420 (8) −1.03 ± 0.14

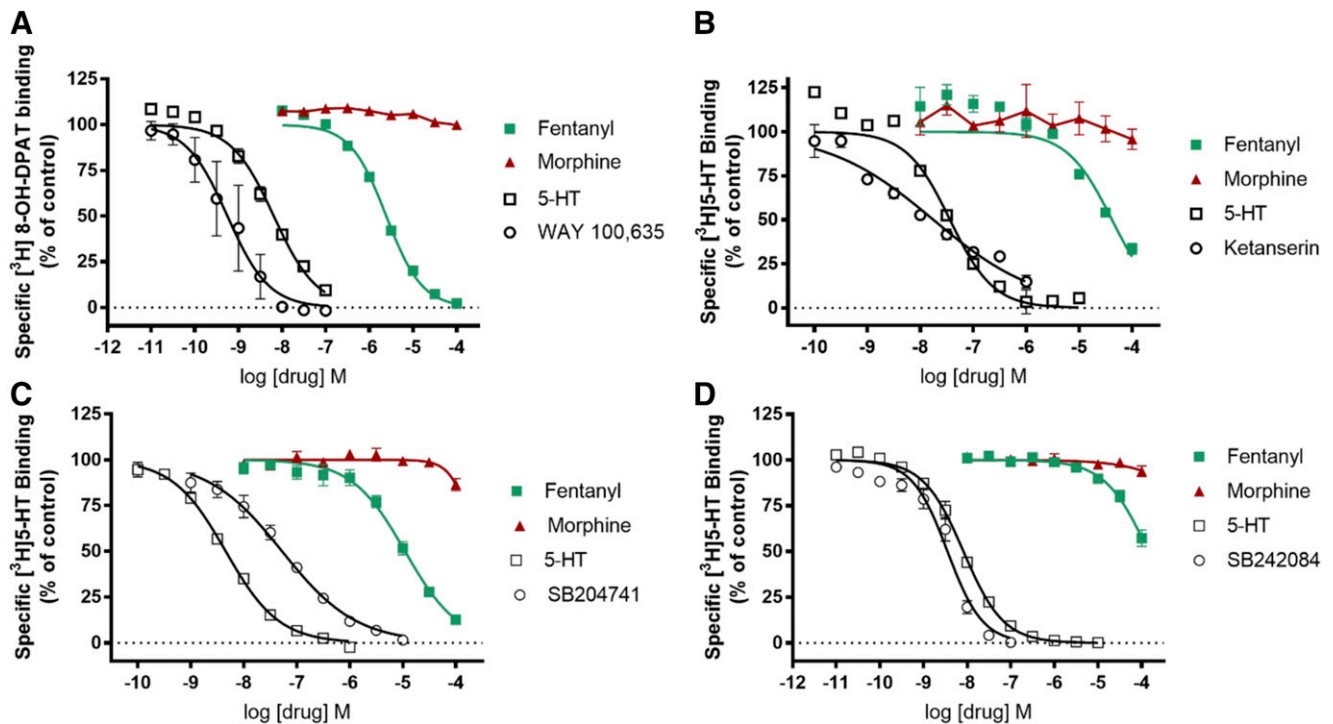n, number of independent experiments, each conducted with duplicate determinations; ND, not determined.

Fig. 8. Drug effects on radioligand binding to serotonin 5HT1A, 5HT2A, 5HT2B, and 5HT2C receptors. (A) 5HT1A receptor ([^{3}H]8-OH-DPAT); (B) 5HT2A receptor ([^{3}H]5-HT); (C) 5HT2B receptor ([^{3}H]5-HT); and (D) 5HT2C receptor ([^{3}H]5-HT). Data shown are the means ± S.E.M. of three to seven experiments.

α_{1D}-Adr (Table 3, $P < 0.0001$), where norepinephrine had its greatest affinity by ~10- to 20-fold over α_{1A}-Adr and α_{1B}-Adr, respectively. The competitive binding pattern of F/FAs suggested by the compounds tested, if consistent among members of this class of drugs/opioids, may allow for the increased availability and coalescence of NE at α_{1D}-Adr and offers an explanation for the consistency of the clinical effects seen with F/FAs. These differences in affinities and availability of norepinephrine (NE) for α_{1D}-Adr binding could play an important role in the effects of F/FAs on noradrenergic system function in the LC (primary noradrenergic system in mammalian central nervous system (CNS)) and cardiovascular system given the key distribution and variations in subtype dominance of α_1-AdRs in these anatomic locations.

Epinephrine had higher affinity for α_{1D}-Adr than fentanyl does ($P < 0.001$) and similar affinities as fentanyl at α_{1A}-Adr and α_{1B}-Adr ($P > 0.05$). Phenylephrine had much lower affinity at α_{1A}-Adr and α_{1B}-Adr ($Ps < 0.01$) but similar affinity at α_{1D}-Adr than fentanyl ($P > 0.05$), and these differences in affinity could affect response to agonist when fentanyl is present. It is noteworthy that carfentanil had greater affinity at the α_{1A}-Adr than epinephrine by nearly twofold. Prazosin and tamsulosin, receptor antagonists, had much higher affinity for [^{3}H]prazosin binding at each receptor subtype than did fentanyl or carfentanil ($Ps < 0.001$) and the Adr agonists (Table 3). However, prazosin had similar affinities for the subtypes, whereas tamsulosin affinities at the subtypes varied (α_{1A}-Adr ≥ α_{1D}-Adr >> α_{1B}-Adr, $P < 0.01$), suggesting that each might be a useful tool for altering noradrenergic function affected by fentanyl, carfentanil, or other F/FAs.

In assays of receptor function, neither morphine, fentanyl, nor carfentanil had agonist activity at any α_1-Adr subtype (Fig. 3; Table 3). The morphine IC$_{50}$ value at blocking

norepinephrine-stimulated IP-1 accumulation was greater than 100 μM at each receptor subtype. Conversely, fentanyl was a relatively weak antagonist at α_{1D}-Adr and inhibited 73% of norepinephrine-mediated IP-1 accumulation. At α_{1A}-Adr and α_{1B}-Adr, fentanyl blocked 100% of norepinephrine-stimulated IP-1 accumulation and had higher potency compared with effects at α_{1D}-Adr (Table 3, $P < 0.01$). Similarly, carfentanil was an antagonist with rank order of potency α_{1B}-Adr > α_{1A}-Adr > α_{1D}-Adr. Norepinephrine and epinephrine had similar potencies ($Ps > 0.05$) and full efficacy at each α_1-Adr subtype, whereas phenylephrine had much lower potency than the neurotransmitters at each receptor subtype ($Ps < 0.001$) and was a partial agonist at α_{1D}-Adr. Prazosin and tamsulosin completely blocked norepinephrine-stimulated IP-1 accumulation, with the same rank order of potencies (α_{1D}-Adr >> α_{1A}-Adr = α_{1B}-Adr, $Ps < 0.05$) (Table 3).

Fentanyl and Morphine Interactions with the VMAT2 and Neurotransmitter Transporters. Table 4 and Fig. 4, A–C indicate that fentanyl and carfentanil were very weak at displacing [^{125}I]RTI-55 binding from the dopamine, serotonin, and norepinephrine transporters, with K_i values ranging from >10 to 69 μM. Morphine's affinity for the binding site at each transporter was even lower, with K_i values at or above 75 μM. Consistent with previous reports, cocaine displaced radioligand binding from the dopamine, serotonin, and norepinephrine transporters (Eshleman et al., 1999), with K_i values ranging from 404 to 1550 nM. Also consistent with previous reports, methamphetamine's K_i values ranged from 2.7 μM at the [^{125}I]RTI-55 binding site on the dopamine transporter to 117 μM at the serotonin transporter. At the VMAT2, fentanyl had a K_i value for displacing [^{3}H] dihydrotetrabenazine (DHTB) of 56 μM, and the carfentanil and morphine K_i values were over 10 and 100 μM, respectively

(Fig. 4D; Table 3). Consistent with previous reports, methamphetamine, a VMAT2 substrate, was very weak at displacing [^{3}H]DHTB binding from the VMAT2, with a K_i value of 684 μM (Eshleman et al., 2013). DHTB, included as a control for the assay, had a K_i of 74 nM.

Because drugs differ between their affinities for radioligand binding sites on transporters and their potencies at inhibiting transporter function, we examined [^{3}H]neurotransmitter uptake by the respective recombinant human transporters and hVMAT2. The data in Table 4 and Fig. 5 indicate that IC$_{50}$ values for morphine were greater than 100 μM, except at the serotonin transporter (>83 μM). Fentanyl, however, had IC$_{50}$ values ranging from 27.5 μM at the norepinephrine transporter and 29.7 μM at the dopamine transporter to >85 μM at the serotonin transporter. Carfentanil had an IC$_{50}$ value of 4.46 μM at the norepinephrine transporter. Importantly, and in contrast to morphine (IC$_{50}$ > 100 μM), the fentanyl IC$_{50}$ value for blocking [^{3}H]5-HT uptake by the hVMAT2 was 911 nM (Fig. 5D), which is more potent than methamphetamine at blocking uptake (4 μM, P < 0.0001, one-way ANOVA Dunnett's multiple comparisons) (Table 4). The K_i/IC$_{50}$ ratio suggests that both fentanyl (ratio 61) and methamphetamine (ratio 164) are binding to a site on the hVMAT2 that is more closely related to transporter function than is the [^{3}H]DHTB binding site (ratio 1.8) (Provencher et al., 2018). Carfentanil had an IC$_{50}$ value of 4.1 μM at the VMAT2.

Fentanyl and Morphine Interactions with Dopamine Receptor Subtypes. The data in Table 5 and Fig. 6 indicate that morphine, at concentrations up to 100 μM, did not displace radioligand binding from any dopamine receptor subtype. Fentanyl, however, had K_i values of ~1 and ~1.7 μM at the dopamine D4.4 [^{3}H]spiperone binding site and the dopamine D1 [^{3}H]SCH23390 binding site, respectively. At the [^{3}H]spiperone binding sites on other D2-like receptors, fentanyl's K_i values were ~15 (D2) and ~12 μM (D3), indicating selectivity for the D4.4 receptor (Fig. 6D; Table 5). Dopamine receptor agonists (SKF38393, quinpirole) and antagonists (SCH23390, butaclamol, haloperidol) had K_i values for radioligand displacement resembling previously reported concentrations (Janowsky et al., 2014).

To determine whether fentanyl or morphine affects dopamine D1 or D4.4 function, we examined their ability to modulate adenylyl cyclase activity that is stimulated (D1) or blocked (D4.4) by these receptors, respectively. Table 6 and Fig. 7A indicate that neither fentanyl nor morphine stimulated adenylyl cyclase activity in C6-D1 cells. However, fentanyl, but not morphine, partially (65.5%) inhibited the activity elicited by 100 nM of dihydrexidine with an IC$_{50}$ value of 27 μM, whereas SCH23390 completely blocked activation with an IC$_{50}$ value of 3.9 nM (Fig. 7B). In HEK-D4.4 cells, neither fentanyl nor morphine had agonist activity as measured by inhibition of forskolin-stimulated adenylyl cyclase activity (Fig. 7C). Fentanyl, not morphine, was a D4.4 antagonist, partially (63%) blocking the quinpirole effect, with an IC$_{50}$ value of 12.7 μM. Haloperidol completely blocked the quinpirole effect, with an IC$_{50}$ value of 152 nM (Fig. 7D; Table 6).

Fentanyl and Morphine Interactions with Serotonin Receptor Subtypes. Table 7 and Fig. 8 indicate the affinities of fentanyl and morphine at the [^{3}H]8-OH-DPAT binding site on the recombinant h5-HT1A receptor and at [^{3}H]5-HT binding sites on the recombinant h5-HT2A, 2B, and 2C receptors. In all cases, morphine K_i values were over 100 μM. However, fentanyl K_i values ranged from ~2.2 μM at the 5-HT1A receptor to 114 μM at the 5-HT2C receptor. Other drugs, selective for the respective receptor subtypes, had effects resembling previously reported K_i values (Eshleman et al., 2013).

Fentanyl and Morphine Interactions with the Recombinant Human CB1 Cannabinoid and NMDA (G2a/G1) Receptors. Table 7 indicates that neither fentanyl nor morphine displaced [^{3}H]CP 55,940 binding to the recombinant hCB1 cannabinoid receptor (K_i > 100 μM) or [^{3}H]MK-801 binding to the recombinant hNMDA (G2a/G1) receptor. Selective agents included in the assays for comparison had K_i values resembling previously reported values (Bresink et al., 1995; Pertwee, 2008a,b).

Discussion

The hypothesis that deaths caused by exposure to F/FAs are not mediated by MORs is based on the following: 1) naloxone availability has not significantly reduced F/FA-related deaths (Baumann et al., 2018); 2) fentanyl metabolites are almost nonexistent in tissue from patients who died of fentanyl overdose, suggesting rapid cardiopulmonary collapse that contrasts with the effects of heroin (Burns et al., 2016); 3) public health data from death scenes and eyewitness reports of F/FA-related deaths show consistent evidence of rapid and atypical death compared with heroin overdose (Somerville et al., 2017); 4) published data on drug effects in animal models and radioligand binding data indicate that fentanyl causes the rapid onset of severe muscle rigidity via ceruspinal fibers innervated/controlled by α_1-Adr postsynaptic receptors (Lui et al., 1989, 1990; Tsou et al., 1989; Fu et al., 1997); 5) the principal effect of high-dose F/FAs is rapid closure of vocal cords followed by rigidity of the chest wall (Scamman, 1983; Bennett et al., 1997); 6) fentanyl isolates the vagal medullary fibers that innervate the vocal cords, contributing to vocal cord closure (Lalley, 2003); and 7) activation of α_1-Adr subtypes facilitates excitatory inputs to medullary airway vagal preganglionic neurons that modulate laryngeal and tracheal musculature (Haxhiu et al., 2003; Ge et al., 2015).

Experimental results herein, comparing the effects of morphine, naloxone, norepinephrine, fentanyl, and carfentanil in the same assay, indicate that pharmacologies differ and that fentanyl binds to α_1-Adrs, add new data on carfentanil-α_1-Adr subtype binding, and indicate that the similar selectivity of fentanyl analogs to α_1-Adr subtypes as a possible underlying mechanism in the lethality of this synthetic opioid family. α_1-Adr subtypes have differing anatomic distributions that further implicate their role in the effects of fentanyl but not morphine. For example, the α_{1D}-Adr, but not α_{1A}-Adr or α_{1B}-Adr subtypes, found predominantly in the large coronary arteries, mediates vasoconstriction (Jensen et al., 2009). The α_{1B}-Adr, found in pulmonary arteries, mediates contraction (Sohn et al., 2005). Norepinephrine had the highest affinity for α_{1D}-Adr compared with α_{1A}-Adr and α_{1B}-Adr (Table 3). A large and rapid fentanyl-induced norepinephrine release (Hicks et al., 1981) should cause α_{1D}-Adr–mediated contraction of coronary arteries, negatively impacting cardiovascular function (Ray et al., 2016). Interestingly, fentanyl was a very weak antagonist at α_{1D}-Adr compared with its ability to antagonize norepinephrine-mediated IP-1 formation at α_{1A}-Adr and

α_{1B}-Adr (Table 3), suggesting a possible focusing of norepinephrine effects on the α_{1D}-Adr subtype when fentanyl is present.

Additionally, fentanyl and carfentanil, but not morphine, blocked VMAT2-mediated neurotransmitter uptake (IC_{50} ~911 nM) but was much weaker at blocking radioligand binding (Table 4). Lobeline, a VMAT2 uptake blocker, has some structural similarities to fentanyl, and fentanyl is more potent than lobeline at blocking VMAT2-mediated [^{3}H]neurotransmitter uptake (lobeline IC_{50} = 4.2 μM) (Provencher et al., 2018). Differing IC_{50} values for uptake and K_i values for binding are consistent with the effects of transporter substrates (Cozzi et al., 2009). The VMAT2 transports neurotransmitter into synaptic vesicles (Erickson et al., 1996); however, preliminary data indicated that the VMAT2 did not transport [^{3}H]fentanyl (data not shown). Thus, fentanyl appears to block uptake but not to displace neurotransmitter from the transporter/vesicle. The resulting increase in intracellular norepinephrine availability and norepinephrine synaptic release via the presynaptic transporter, coupled with fentanyl blockade of α_{1A}- and α_{1B}-Adr (the α_{1D}-Adr has relatively lower affinity for fentanyl), could result in more selective α_{1D}-Adr stimulation, consistent with deleterious α_{1D}-mediated consequences, including coronary artery vasospasm, as mentioned above.

Dopamine receptors had differential affinity for fentanyl, with the D1 and D4.4 receptors having the highest affinity, ~1 μM (Table 5), and fentanyl was a weak antagonist at both receptors (Table 6). In agreement with previous reports, fentanyl's potency at blocking D1 receptor–mediated cAMP accumulation (Govoni et al., 1975) was similar to fentanyl's affinity at blocking [^{3}H]SCH 23390 binding to the D1 receptor. Lalley (2005a,b) suggested that dopamine D1 receptor agonists might reverse opioid-induced respiratory depression but not antinociception, whereas antagonists enhance respiratory depression. Therefore, fentanyl-mediated blockade of the D1 receptor subtypes should increase MOR-mediated respiratory depression, necessitating increased administration of naloxone, consistent with findings related to fentanyl overdose.

Previous reports also used [^{3}H]8-OH-DPAT to characterize fentanyl's effects at 5HT1A receptors and obtained almost identical results (K_i ~2 μM) (Rickli et al., 2018). However, we report that fentanyl had micromolar affinity (31 μM) at the 5HT2A receptor as measured by using an agonist, [^{3}H]5-HT, whereas Rickli et al. (2018) obtained a K_i value of 1.3 μM by using the antagonist [^{3}H]ketanserin. Differences in affinity for the binding sites could be because of the use of agonist versus antagonist ligand. We found no reports indicating direct effects of fentanyl on receptor function that could corroborate any differences in affinity caused by differences in radioligand. Fentanyl had very low affinity for the 5HT2C receptor, regardless of radioligand, and our data (Table 7) are the first indication of low affinity of fentanyl at the recombinant human 5HT2B receptor.

In agreement with a previous report (Fernández-Fernández et al., 2014) indicating that fentanyl did not displace [^{3}H]CP55,940 binding from CB1 receptors in human cortical preparations, neither fentanyl nor morphine displaced [^{3}H]CP55,940 binding from the recombinant human receptor (Table 7). Additionally, neither fentanyl nor morphine blocked [^{3}H]MK-801 binding to recombinant NMDA receptors (G2a/G1), in agreement with a report describing a rat cortical wedge

preparation (Ebert et al., 1998). The low affinity precluded functional tests, but both fentanyl and morphine, at high micromolar concentrations, block the function of NMDA channels of various subunit compositions expressed in *Xenopus* oocytes (Yamakura et al., 1999).

Whether the K_i and IC_{50} values described above are relevant to the symptoms of fentanyl overdose depend on pharmacokinetic assumptions. Fentanyl is lipophilic, and calculated brain lipid concentrations can reach almost 3 mM (Stone and DiFazio, 1988). The high octanol/water partition coefficient for fentanyl (9550) and carfentanil (~>13,000) suggests that toxic brain interstitial concentrations in the high nanomolars to low micromolars range are relevant (Stone and DiFazio, 1988). However, calculations based on plasma drug concentrations suggest that brain concentrations are much lower (Kalvass et al., 2007; Heiskanen et al., 2015). Sheep models have demonstrated significant first pass peak concentrations reaching the brain after intravenous drug administration that may be up to 4000-times greater than plasma concentrations within the first minute of circulation (Upton, 1996). The pharmacokinetic assumptions that illicit fentanyl administration results in very high (millimolars) concentrations in various compartments suggest that our data (low micromolars K_i and IC_{50} values) at various receptors and transporters are pharmacologically relevant and contribute to the differences between morphine and fentanyl in clinical symptoms and outcomes.

The relevance of these findings is significant given the incidence of deaths from F/FAs. High doses of F/FAs in animal models increase signal output from the LC, causing severe and sustained chest wall rigidity and are mediated by the direct interaction of noradrenaline and α_1-Adr receptors (Lui et al., 1989). Similarly, LC output controls medullary vagal motor fibers innervating the airway, whereas fentanyl selectively activates vagal motor fibers (Haxhiu et al., 2003; Lalley, 2003). These reports and our data support plausible mechanisms for increased noradrenergic activity and selective non-MOR receptor/VMAT2 transporter blockade that is the prerequisite for synthetic opioid-induced overdose, with resulting laryngospasm, cardiovascular, and secondary hepatic compromise (Yasuda et al., 1978; Scamman, 1983; Lui et al., 1989, 1990, 1993, 1995; Bennett et al., 1997; Burns et al., 2016; Somerville et al., 2017; Torralva and Janowsky, 2019). These mechanisms appear to be distinct from the effects of F/FAs at MORs (Sokoll et al., 1972).

F/FAs increase norepinephrine in peripheral circulation (Thomson et al., 1988). However, F/FAs, and in fact all opioids, decrease norepinephrine release in the CNS (Aghajanian, 1982). Our new data demonstrate two mechanisms by which fentanyl may alter norepinephrine disposition: 1) fentanyl blocked intracellular vesicular reuptake of neurotransmitter (Fig. 5), increasing their cytoplasmic concentrations; and 2) fentanyl selectively blocked α_1-Adr receptor subtypes (Table 3) in a manner that isolates and focuses noradrenergic activity on the α_{1D}-Adr subtype (Fig. 3), where norepinephrine has its highest affinity.

Our hypothesis concerning a nonopioid fentanyl-modulated pathway has relevance for the current fentanyl-driven opioid crisis, in which the increased deaths and reduced sensitivity to naloxone may be because of acute vocal cord closure and cardiovascular dysfunction mediated by noradrenergic activity at α_{1D}-Adr receptors, where opioid antagonists would have little effect (Willette and Sapru, 1982; Torralva and Janowsky, 2019). These data suggest the underlying mechanisms for FIRE and indicate new directions for development of

supplementary modes of emergency treatment and strategic interventional targets (e.g., α_1-Adr receptor subtypes) that may improve survival from F/FA exposure.

In conclusion, the current novel data may be relevant to the development of therapeutics targeting the underlying mechanism of the adverse effects and deaths associated with F/FAs. The affinity and effects of fentanyl at α_1-Adr subtypes and the VMAT2 differ significantly from morphine. Thus, profiling of new fentanyl analogs and synthetic opioids against the receptor panel described here could help to identify therapeutic candidates with fewer adverse clinical effects and indicate strategic intervention points for the lethal mechanisms of these compounds.

Authorship Contributions

Participated in research design: Torralva, Eshleman, Schutzer, Janowsky.

Conducted experiments: Eshleman, Swanson, Schmachtenberg, Bloom, Wolfrum, Reed.

Performed data analysis: Eshleman, Swanson, Schmachtenberg, Schutzer, Bloom, Wolfrum, Reed, Janowsky.

Wrote or contributed to the writing of the manuscript: Torralva, Eshleman, Swanson, Schmachtenberg, Schutzer, Bloom, Wolfrum, Reed, Janowsky.

References

Aghajanian GK (1982) Central noradrenergic neurons: a locus for the functional interplay between alpha-2 adrenoceptors and opiate receptors. *J Clin Psychiatry* **43**:20–24.

Baumann MH, Kopajtic TA, and Madras BK (2018) Pharmacological research as a key component in mitigating the opioid overdose crisis. *Trends Pharmacol Sci* **39**:995–998.

Bennett JA, Abrams JT, Van Riper DF, and Horrow JC (1997) Difficult or impossible ventilation after sufentanil-induced anesthesia is caused primarily by vocal cord closure. *Anesthesiology* **87**:1070–1074.

Bergström KA, Jolkkonen J, Kuikka JT, Akerman KK, Viinamäki H, Airaksinen O, Länsimies E, and Tiihonen J (1998) Fentanyl decreases beta-CIT binding to the dopamine transporter. *Synapse* **29**:413–415.

Bresink I, Danysz W, Parsons CG, and Mutschler E (1995) Different binding affinities of NMDA receptor channel blockers in various brain regions--indication of NMDA receptor heterogeneity. *Neuropharmacology* **34**:533–540.

Burns G, DeRienz RT, Baker DD, Casavant M, and Spiller HA (2016) Could chest wall rigidity be a factor in rapid death from illicit fentanyl abuse? *Clin Toxicol (Phila)* **54**:420–423.

Cheng Y and Prusoff WH (1973) Relationship between the inhibition constant (K1) and the concentration of inhibitor which causes 50 per cent inhibition (I50) of an enzymatic reaction. *Biochem Pharmacol* **22**:3099–3108.

Chesser R, Pardi J, Concheiro M, and Cooper G (2019) Distribution of synthetic opioids in postmortem blood, vitreous humor and brain. *Forensic Sci Int* **305**:109999.

Cozzi NV, Gopalakrishnan A, Anderson LL, Feih JT, Shulgin AT, Daley PF, and Ruoho AE (2009) Dimethyltryptamine and other hallucinogenic tryptamines exhibit substrate behavior at the serotonin uptake transporter and the vesicle monoamine transporter. *J Neural Transm (Vienna)* **116**:1591–1599.

de Waal PW, Shi J, You E, Wang X, Melcher K, Jiang Y, Xu HE, and Dickson BM (2020) Molecular mechanisms of fentanyl mediated β-arrestin biased signaling. *PLOS Comput Biol* **16**:e1007394.

Ebert B, Andersen S, Hjeds H, and Dickenson AH (1998) Dextropropoxyphene acts as a noncompetitive N-methyl-D-aspartate antagonist. *J Pain Symptom Manage* **15**:269–274.

Erickson JD, Schafer MK, Bonner TI, Eiden LE, and Weihe E (1996) Distinct pharmacological properties and distribution in neurons and endocrine cells of two isoforms of the human vesicular monoamine transporter. *Proc Natl Acad Sci USA* **93**:5166–5171.

Eshleman AJ, Carmolli M, Cumbay M, Martens CR, Neve KA, and Janowsky A (1999) Characteristics of drug interactions with recombinant biogenic amine transporters expressed in the same cell type. *J Pharmacol Exp Ther* **289**:877–885.

Eshleman AJ, Wolfrum KM, Hatfield MG, Johnson RA, Murphy KV, and Janowsky A (2013) Substituted methcathinones differ in transporter and receptor interactions. *Biochem Pharmacol* **85**:1803–1815.

Eshleman AJ, Wolfrum KM, Reed JF, Kim SO, Johnson RA, and Janowsky A (2018) Neurochemical pharmacology of psychoactive substituted N-benzylphenethylamines: high potency agonists at 5-HT$_{2A}$ receptors. *Biochem Pharmacol* **158**:27–34.

Farrens DL, Dunham TD, Fay JF, Dews IC, Caldwell J, and Nauert B (2002) Design, expression, and characterization of a synthetic human cannabinoid receptor and cannabinoid receptor/ G-protein fusion protein. *J Pept Res* **60**:336–347.

Fernández-Fernández C, Callado LF, Girón R, Sánchez E, Erdozain AM, López-Moreno JA, Morales P, Rodríguez de Fonseca F, Fernández-Ruiz J, Goya P, et al. (2014) Combining rimonabant and fentanyl in a single entity: preparation and pharmacological results. *Drug Des Devel Ther* **8**:263–277.

Fu MJ, Tsen LY, Lee TY, Lui PW, and Chan SH (1997) Involvement of ceru:lospinal glutamatergic neurotransmission in fentanyl-induced muscular rigidity in the rat. *Anesthesiology* **87**:1450–1459.

Ge D, Yan X, Guo Y, Chen X, Guan R, Chen Y, Qiu D, and Wang J (2015) Activation of alpha1-adrenoceptors facilitates excitatory inputs to medullary airway vagal preganglionic neurons. *J Appl Physiol (1985)* **119**:686–695.

Govoni S, Kumakura K, Spano PF, Tonon GC, and Trabucchi M (1975) Interaction of narcotic analgesics with dopamine receptors in rat brain. *Pharmacol Res Commun* **7**:95–100.

Grant ER, Bacskai BJ, Pleasure DE, Pritchett DB, Gallagher MJ, Kendrick SJ, Kricka LJ, and Lynch DR (1997) N-methyl-D-aspartate receptors expressed in a nonneuronal cell line mediate subunit-specific increases in free intracellular calcium. *J Biol Chem* **272**:647–656.

Grell FL, Koons RA, and Denson JS (1970) Fentanyl in anesthesia: a report of 500 cases. *Anesth Analg* **49**:523–532.

Haxhiu MA, Kc P, Neziri B, Yamamoto BK, Ferguson DG, and Massari VJ (2003) Catecholaminergic microcircuitry controlling the output of airway-related vagal preganglionic neurons. *J Appl Physiol (1985)* **94**:1999–2009.

Hedegaard H, Bastian BA, Tinidad JP, Spencer M, and Warner M (2018) Drugs most frequently involved in drug overdose deaths: United States, 2011-2016, *Natl Vital Stat Rep* **67**, pp 1–14.

Heiskanen T, Langel K, Gunnar T, Lillsunde P, and Kalso EA (2015) Opioid concentrations in oral fluid and plasma in cancer patients with pain. *J Pain Symptom Manage* **50**:524–532.

Hicks HC, Mowbray AG, and Yhap EO (1981) Cardiovascular effects of and catecholamine responses to high dose fentanyl-O2 for induction of anesthesia in patients with ischemic coronary artery disease. *Anesth Analg* **60**:563–568.

Hustveit O (1994) Binding of fentanyl and pethidine to muscarinic receptors in rat brain. *Jpn J Pharmacol* **64**:57–59.

Jannetto PJ, Helander A, Garg U, Janis GC, Goldberger B, and Ketha H (2019) The fentanyl epidemic and evolution of fentanyl analogs in the United States and the European union. *Clin Chem* **65**:242–253.

Janowsky A, Eshleman AJ, Johnson RA, Wolfrum KM, Hinrichs DJ, Yang J, Zabriskie TM, Smilkstein MJ, and Riscoe MK (2014) Mefloquine and psychotomimetics share neurotransmitter receptor and transporter interactions in vitro. *Psychopharmacology (Berl)* **231**:2771–2783.

Jensen BC, Swigart PM, Laden ME, DeMarco T, Hoopes C, and Simpson PC (2009) The alpha-1D Is the predominant alpha-1-adrenergic receptor subtype in human epicardial coronary arteries. *J Am Coll Cardiol* **54**:1137–1145.

Jiwa N, Sheth H, and Silverman R (2018) Naloxone-induced non-cardiogenic pulmonary edema: a case report. *Drug Saf Case Rep* **5**:20.

Kalvass JC, Olson ER, Cassidy MP, Selley DE, and Pollack GM (2007) Pharmacokinetics and pharmacodynamics of seven opioids in P-glycoprotein-competent mice: assessment of unbound brain EC50,u and correlation of in vitro, preclinical, and clinical data. *J Pharmacol Exp Ther* **323**:346–355.

Katchman AN, McGroary KA, Kilborn MJ, Kornick CA, Manfredi PL, Woosley RL, and Ebert SN (2002) Influence of opioid agonists on cardiac human ether-a-go-go-related gene K(+) currents. *J Pharmacol Exp Ther* **303**:688–694.

Lalley PM (2003) Mu-opioid receptor agonist effects on medullary respiratory neurons in the cat: evidence for involvement in certain types of ventilatory disturbances. *Am J Physiol Regul Integr Comp Physiol* **285**:R1287–R1304.

Lalley PM (2005a) D1-dopamine receptor agonists prevent and reverse opiate depression of breathing but not antinociception in the cat. *Am J Physiol Regul Integr Comp Physiol* **289**:R45–R51.

Lalley PM (2005b) D1-dopamine receptor blockade slows respiratory rhythm and enhances opioid-mediated depression. *Respir Physiol Neurobiol* **145**:13–22.

Lui PW, Chang GJ, Lee TY, and Chan SH (1993) Antagonization of fentanyl-induced muscular rigidity by denervation of the coerulospinal noradrenergic pathway in the rat. *Neurosci Lett* **157**:145–148.

Lui PW, Lee TY, and Chan SH (1989) Involvement of locus coeruleus and noradrenergic neurotransmission in fentanyl-induced muscular rigidity in the rat. *Neurosci Lett* **96**:114–119.

Lui PW, Lee TY, and Chan SH (1990) Involvement of coerulospinal noradrenergic pathway in fentanyl-induced muscular rigidity in rats. *Neurosci Lett* **108**:183–188.

Lui PW, Tsen LY, Fu MJ, Yeh CP, Lee TY, and Chan SH (1995) Inhibition by intrathecal prazosin but not yohimbine of fentanyl-induced muscular rigidity in the rat. *Neurosci Lett* **201**:167–170.

Martin DC, Introna RP, and Aronstam RS (1991) Fentanyl and sufentanil inhibit agonist binding to 5-HT1A receptors in membranes from the rat brain. *Neuropharmacology* **30**:323–327.

McClain DA and Hug CC Jr. (1980) Intravenous fentanyl kinetics. *Clin Pharmacol Ther* **28**:106–114.

Peng PW and Sandler AN (1999) A review of the use of fentanyl analgesia in the management of acute pain in adults. *Anesthesiology* **90**:576–599.

Pertwee RG (2008a) The diverse CB1 and CB2 receptor pharmacology of three plant cannabinoids: delta9-tetrahydrocannabinol, cannabidiol and delta9-tetrahydrocannabivarin. *Br J Pharmacol* **153**:199–215.

Pertwee RG (2008b) Ligands that target cannabinoid receptors in the brain: from THC to anandamide and beyond. *Addict Biol* **13**:147–159.

Provencher BA, Eshleman AJ, Johnson RA, Shi X, Kryatova O, Nelson J, Tian J, Gonzalez M, Meltzer PC, and Janowsky A (2018) Synthesis and discovery of arylpiperidinylquinazolines: new inhibitors of the vesicular monoamine transporter. *J Med Chem* **61**:9121–9131.

Ray WA, Chung CP, Murray KT, Hall K, and Stein CM (2016) Prescription of long-acting opioids and mortality in patients with chronic noncancer pain. *JAMA* **315**:2415–2423.

Rickli A, Liakoni E, Hoener MC, and Liechti ME (2018) Opioid-induced inhibition of the human 5-HT and noradrenaline transporters in vitro: link to clinical reports of serotonin syndrome. *Br J Pharmacol* **175**:532–543.

Scamman FL (1983) Fentanyl-O2-N2O rigidity and pulmonary compliance. *Anesth Analg* **62**:332–334.

Shi X, Walter NA, Harkness JH, Neve KA, Williams RW, Lu L, Belknap JK, Eshleman AJ, Phillips TJ, and Janowsky A (2016) Genetic polymorphisms affect mouse and human trace amine-associated receptor 1 function. *PLoS One* **11**:e0152581.

Slavova S, Costich JF, Bunn TL, Luu H, Singleton M, Hargrove SL, Triplett JS, Quesinberry D, Ralston W, and Ingram V (2017) Heroin and fentanyl overdoses in Kentucky: epidemiology and surveillance. *Int J Drug Policy* **46**:120–129.

Sohn JT, Ding X, McCune DF, Perez DM, and Murray PA (2005) Fentanyl attenuates alpha1B-adrenoceptor-mediated pulmonary artery contraction. *Anesthesiology* **103**:327–334.

Sokoll MD, Hoyt JL, and Gergis SD (1972) Studies in muscle rigidity, nitrous oxide, and narcotic analgesic agents. *Anesth Analg* **51**:16–20.

Somerville NJ, O'Donnell J, Gladden RM, Zibbell JE, Green TC, Younkin M, Ruiz S, Babakhanlou-Chase H, Chan M, Callis BP, et al. (2017) Characteristics of fentanyl overdose - Massachusetts, 2014-2016. *MMWR Morb Mortal Wkly Rep* **66**:382–386.

Stanley TH (2014) The fentanyl story. *J Pain* **15**:1215–1226.

Stone DJ and DiFazio CA (1988) Anesthetic action of opiates: correlations of lipid solubility and spectral edge. *Anesth Analg* **67**:663–666.

Streisand JB, Bailey PL, LeMaire L, Ashburn MA, Tarver SD, Varvel J, and Stanley TH (1993) Fentanyl-induced rigidity and unconsciousness in human volunteers. Incidence, duration, and plasma concentrations. *Anesthesiology* **78**:629–634.

Thomson IR, Hudson RJ, Rosenbloom M, and Torchia MG (1988) Catecholamine responses to anesthetic induction with fentanyl and sufentanil. *J Cardiothorac Anesth* **2**:18–22.

Torralva R and Janowsky A (2019) Noradrenergic mechanisms in fentanyl-mediated rapid death explain failure of naloxone in the opioid crisis. *J Pharmacol Exp Ther* **371**:453–475.

Traynor JR and Nahorski SR (1995) Modulation by mu-opioid agonists of guanosine-5′-O-(3-[35S]thio)triphosphate binding to membranes from human neuroblastoma SH-SY5Y cells. *Mol Pharmacol* **47**:848–854.

Tschirhart JN, Li W, Guo J, and Zhang S (2019) Blockade of the human ether A-go-go-related gene (hERG) potassium channel by fentanyl. *Mol Pharmacol* **95**:386–397.

Tsou MY, Lui PW, Lee TY, Pan JT, and Chan SH (1989) Differential effects of prazosin and yohimbine on fentanyl-induced muscular rigidity in rats. *Neuropharmacology* **28**:1163–1168.

Upton RN (1996) A model of the first pass passage of drugs from i.v. injection site to the heart--parameter estimates for lignocaine in the sheep. *Br J Anaesth* **77**:764–772.

Vasudevan L, Vandeputte M, Deventer M, Wouters E, Cannaert A, and Stove CP (2020) Assessment of structure-activity relationships and biased agonism at the Mu opioid receptor of novel synthetic opioids using a novel, stable bio-assay platform. *Biochem Pharmacol* **177**:113910.

Willette RN and Sapru HN (1982) Pulmonary opiate receptor activation evokes a cardiorespiratory reflex. *Eur J Pharmacol* **78**:61–70.

Yamakura T, Sakimura K, and Shimoji K (1999) Direct inhibition of the N-methyl-D-aspartate receptor channel by high concentrations of opioids. *Anesthesiology* **91**:1053–1063.

Yamanoue T, Brum JM, Estafanous FG, Khairallah PA, and Ferrario CM (1993) Fentanyl attenuates porcine coronary arterial contraction through M3-muscarinic antagonism. *Anesth Analg* **76**:382–390.

Yang M, Reese J, Cotecchia S, and Michel MC (1998) Murine alpha1-adrenoceptor subtypes. I. Radioligand binding studies. *J Pharmacol Exp Ther* **286**:841–847.

Yasuda I, Hirano T, Yusa T, and Satoh M (1978) Tracheal constriction by morphine and by fentanyl in man. *Anesthesiology* **49**:117–119.

Address correspondence to: Aaron Janowsky, Research Service (R&D22), VA Portland Health Care System, 3710 S.W. U.S. Veterans Hospital Rd., Portland OR 97239. E-mail: janowsky@ohsu.edu